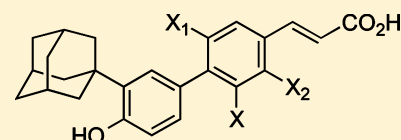


Analogues of Orphan Nuclear Receptor Small Heterodimer Partner Ligand and Apoptosis Inducer (*E*)-4-[3-(1-Adamantyl)-4-hydroxyphenyl]-3-chlorocinnamic Acid. 2. Impact of 3-Chloro Group Replacement on Inhibition of Proliferation and Induction of Apoptosis of Leukemia and Cancer Cell LinesZebin Xia,[†] Ricardo G. Correa,[†] Jayanta K. Das,[‡] Lulu Farhana,[‡] David J. Castro,[†] Jinghua Yu,[†] Robert G. Oshima,[†] Joseph A. Fontana,[‡] John C. Reed,[†] and Marcia I. Dawson^{*,†}[†]Cancer Center, Sanford-Burnham Medical Research Institute, La Jolla, California 92037, United States[‡]Department of Veterans Affairs Medical Center and Wayne State University School of Medicine, Detroit, Michigan 48201, United States

Supporting Information

ABSTRACT: The parent phenol of adapalene and its (*E*)-cinnamic acid analogue were found to induce cancer cell apoptosis but cause adverse systemic effects when administered to mice. In contrast, their respective 5-Cl- and 3-Cl-substituted analogues had their adverse effects mitigated without a comparable loss of cancer cell inhibitory activity. As a result, pharmacologic space in this region of the cinnamic phenyl ring scaffold was explored. Various substituents were introduced, and their effects on cancer cell proliferation and viability were evaluated. Cinnamic acids having 3-Br, CN, NO₂, NH₂, OMe, and N₃ groups had activity comparable to that of 4-[3'-(1-adamantyl)-4'-hydroxyphenyl]-3-chlorocinnamic acid. A comparative molecular field analysis study indicated that introduction of an H-bond acceptor at position 3 of the central phenyl ring would favor inhibition of leukemia cell viability, and docking suggested its hydrogen bonding with a polar group in a small heterodimer partner homology model. The 3-CN, NO₂, NH₂, and OH analogues also inhibited MMTV-Wnt1 murine mammary stem cell viability.



X = H, Cl, Br, Me, CH₂OH, CF₃,
CN, CO₂Me, OMe, OEt, OH,
NO₂, NH₂, N₃
X₁ = H, Cl, Me, OMe
X₂ = H, F, Cl, Br

INTRODUCTION

We discovered that 5-Cl-AHPN (**3**) and 3-Cl-AHPC (**8**) (Figure 1) are ligands of the orphan nuclear receptor (NR) small heterodimer partner (SHP) on the basis of their competitive binding with the 5,5'-tritiated analogue of SHP ligand AHPN (**1**).¹ SHP is one of two unique orphan nuclear receptors in having only a ligand-binding domain (LBD) through which it acts to regulate cell processes such as survival, DNA methylation, and metabolism.^{2–4} Although a crystal structure of SHP has not been reported, a homology model was derived from the structure [Protein Data Bank (PDB) entry 1G2N] of the LBD of ultraspiracle (USP) protein,⁵ which is the insect homologue of the vertebrate orphan NR retinoid X receptor (RXR).⁶ This model, which has been partially validated by mutagenesis,⁷ has the canonical NR LBD structure of 12 sandwiched α -helices, a short β -sheet between helices H5 and H6, a H12 containing a ligand-dependent activation function 2 (AF-2), and a putative ligand-binding pocket (LBP) to which a USP ligand could be docked.⁶ This model also revealed that NR box or coactivator (CoA) motifs (LXXLL, X = unspecified) were located in helical regions corresponding to NR LBD H1, H6, and H10. The NR motifs permit a CoA protein to interact with the NR AF-2 surface generated by NR H3, H4, and H12, thereby allowing the NR–CoA complex bound to DNA to recruit the transcriptional complex. In contrast, binding by a SHP

NR box to the AF-2 surface generally represses NR transactivational activity. While a natural ligand for SHP has not been reported, our studies showed that small molecules such as **1** and **8** (Figure 1) by interacting with SHP induced SHP to interact with the mSin3A multiprotein repressor complex,¹ thereby modifying expression of several genes, including c-Fos and c-Jun,⁸ leading to activation of JNK and NF- κ B signaling pathways and resulting in apoptosis of cancer and leukemia cell lines.^{8–10}

Without a structure of SHP available, ligand design has relied on indirect methods such as structure–activity analysis and docking of candidates to the homology model. The prototype for SHP ligands was the aromatic retinoid 6-[3'-(1-adamantyl)-4'-hydroxyphenyl]-2-naphthalenecarboxylic acid (AHPN/CD437, **1**), the parent phenol of the anti-acne drug adapalene. The retinoid-like adverse effects of **1** were mitigated in the 4-aryl 3-chlorocinnamic acid **8**, which was unable to transcriptionally activate the retinoic acid nuclear receptors (RARs).¹¹ Molecular dynamics of the more rigid 5-chloronaphthalenecarboxylic acid analogue (**3**) of **8** suggested why the chloro group on the central aryl ring ortho to the diaryl bond would interfere in the docking of **3** (Figure 1; X = Cl in Table 1) to

Received: August 26, 2011

Published: December 2, 2011

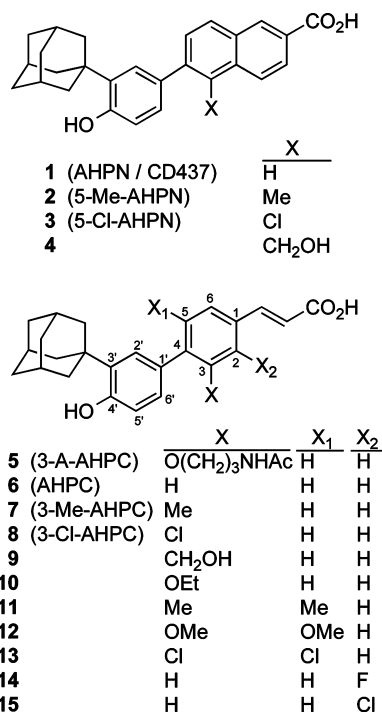


Figure 1. Structures of the adamantyl-substituted retinoid-related AHPN series: AHPN/CD437 (**1**), 5-Me-AHPN (**2**), 5-Cl-AHPN (**3**), and **4**. Structures of the similarly substituted AHPC series: 3-A-AHPC (**5**), AHPC (**6**), 3-Me-AHPC (**7**), 3-Cl-AHPC (**8**), and **9–15**.

the agonist conformation of the RAR γ LBD (PDB entry 3LBD).¹² With the naphthalenecarboxylate group of **3** anchored by ionic and/or H-bonding interactions with the LBD H5 R278 side chain in the RAR ligand-binding pocket, the larger 5-Cl group caused the torsion angle between the aryl rings of **3** to increase so that its 1-adamantyl group (1-Ad) clashed with side chains in the agonist position of H11, thereby preventing H12 from forming the AF-2 surface. Fortunately, the new orientation of the aryl rings did not prevent **3** and **8** from inducing cancer cell apoptosis.¹¹

To explore chemical space about the 5-Cl group of **3** and the 3-Cl group of analogue **8**, we had previously synthesized and evaluated a limited series of analogues. Their abilities to inhibit the proliferation and induce the apoptosis of all-*trans*-retinoic acid (ATRA)-resistant human HL-60R myeloid leukemia and MDA-MB-231 breast cancer cell lines at 1.0 and 5.0 μ M are summarized in Table 1. The growth inhibitory and apoptotic activities of several compounds from these initial studies indicated that introducing particular groups at position 5 of naphthalene-2-carboxylic acid **1** and position 3 of cinnamic acid **6** negatively impacted efficacy. Their analogues, **2** and **7**, respectively, with a methyl group at these positions were less active than the parent structures, whereas **3** and **8** with a chloro group, which was only 3 Å³ smaller (13.5%) in volume than the methyl group, had these activities partially restored.¹¹ In contrast, introduction of larger groups such as hydroxymethyl and ethoxy in **4** and **10**, respectively, caused the loss of both activities. Moreover, the introduction of two methyl and methoxy substituents at positions 3 and 5 of the central phenyl ring (**11** and **12**, respectively), both of which are ortho to the diaryl bond, further diminished activity against MDA-MB-231 cell proliferation, whereas introducing 3,5-dichloro groups (**13**) did not impact MDA-MB-231 growth inhibition but did

diminish HL-60R cell apoptosis compared to that with **8**. Shifting the 3-Cl group to position 2 of the cinnamic acid ring in **15** ($X_2 = \text{Cl}$) caused a loss of activity against both cell lines (Table 1), whereas the corresponding 2-F group of **14** ($X_2 = \text{F}$) with a volume of 10.7 Å³ weakened only MDA-MB-231 growth inhibition but did not affect HL-60R apoptosis induction. Docking studies described below now suggest reasons for these differences.

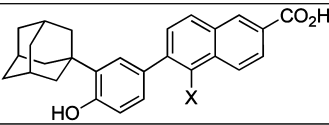
These previous results suggested that further increasing the volume of the central ring substituent ortho to the diaryl bond would inversely correlate with levels of growth inhibition and apoptosis induction. As a corollary, those analogues with smaller substituents at position 3 would interact with SHP but those with larger volumes would not. To more thoroughly explore space in this region, these studies focused on additional analogues of **6** because of their relative ease of synthesis. Initially, evaluations employed KG-1 AML cells and then were extended to OCI-AML2 AML, K562 chronic myeloid leukemia (CML), and MOLT4 T-cell acute lymphoblastic leukemia (T-ALL) cell lines for which the analogue dose response was investigated. Several of the more potent analogues were also evaluated using the murine MMTV-Wnt1 mammary stem cell line in which the Wnt1 oncogene had been overexpressed.

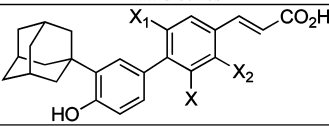
RESULTS

Design and Chemical Synthesis. Computational studies indicated that **8** assumed two poses when docked to the SHP model.¹³ Both poses suggested that the carboxylate group of **8** could have ionic interactions with the side chain of R238 in SHP helix H11, its phenolic hydroxyl could form an H- π bond with the phenyl ring of F96 in H5, and its 1-adamantyl group could have van der Waals and/or hydrophobic contacts with L97, L100, A145, and W148. In contrast, the cinnamyl ring of **8** occupied orthogonal positions so that the 3-Cl group was directed toward LBP hydrophobic residues or toward the polar side chains of T55 and C56 in H3. This second orientation suggested a possible H-bond interaction with the threonine hydroxyl group and/or cysteine sulfhydryl group. To explore the importance of the substituent at position 3 with respect to volume and electrostatic properties and its subsequent impact on ligand orientation in the SHP LBP, analogues **46–52**, **57**, **59**, and **61** with various substituents at position 3 were designed, synthesized (Schemes 1 and 2), and evaluated (Table 2). In addition, the effect on activity of a substituent at cinnamic acid ring position 6, which is ortho to the cinnamic acid double bond, was explored in **63** ($X_1 = \text{Br}$), and that of restricting the aryl rings to a planar orientation was investigated in tricyclic carbazoles **66** and **69**, in which a common nitrogen atom and the diaryl bond combined to restrict ring rotation.

The general route to the 3-substituted analogues of **8** involved constructing a series of (*E*)-cinnamate intermediates by a Mizoroki-Heck vinyl-aryl coupling¹⁴ of 3,4-disubstituted phenyl halides with ethyl acrylate or by a Wittig reaction^{15,16} on 3,4-disubstituted benzaldehydes. After suitable functionalization followed by the Suzuki-Miyaura diaryl coupling,¹⁷ suitably-functionalized cinnamates with 3-(1-adamantyl)-4-benzyloxyphenylboronic acid (**34**) were used to introduce the central diaryl bond (Schemes 1 and 2). One-step procedures were used to prepare four of the five precursors required for constructing the required 3,4-disubstituted cinnamates (Scheme 1). Thus, diazotization of aniline **16** at -5 to 0 °C and treatment with potassium iodide at 22 – 100 °C afforded 4-bromo-3-trifluoromethylphenyl iodide (**17**) required for intermediate **25**.

Table 1. Effects of a Substituent on the Central Aryl Ring on Analogue Activity Compared to That of the 5-Chloro Group of 1 and the 3-Chloro Group of 8 in Terms of Human Leukemia and Breast Cancer Cell Growth Inhibition and Apoptosis Induction^a

AHPN series		growth inhibition after treatment (%) ^b				apoptosis (%) after treatment time ^b					
		KG-1 AML at 48 h		MDA-MB-231 breast cancer at 96 h		HL-60R leukemia at 24 h		KG-1 AML at 48 h		MDA-MB-231 breast cancer at 96 h	
compound	X ^c	1.0 μM	5.0 μM	1.0 μM	2.0 μM	0.1 μM	1.0 μM	1.0 μM	5.0 μM	1.0 μM	2.0 μM
1	H	46 ^e	64 ^e	73 ^d	98 ^d	26 ^f	46 ^e				
2	Me	91 ^d	94 ^d	28 ^f	43 ^e	29 ^f	70 ^e	50 ^e	72 ^d	28 ^f	43 ^e
3	Cl	41 ^e	66 ^e	62 ^e	94 ^d	21 ^g	41 ^e				
4	CH ₂ OH	1 ^g	1 ^g	0 ^g	74 ^d						

AHPC series				growth inhibition after treatment (%) ^b				apoptosis (%) after treatment time ^b					
				KG-1 AML at 48 h		MDA-MB-231 breast cancer at 96 h		HL-60R leukemia at 24 h		KG-1 AML at 48 h		MDA-MB-231 breast cancer at 96 h	
compound	X ^c	X ₁ ^f	X ₂ ^c	1.0 μM	5.0 μM	1.0 μM	2.0 μM	0.1 μM	1.0 μM	1.0 μM	5.0 μM	1.0 μM	2.0 μM
6	H	H	H	53 ^e	57 ^e	90 ^d	98 ^d	23 ^f	42 ^e	53 ^e	58 ^e		
7	Me	H	H	30 ^f	49 ^e	10 ^g	95 ^d	30 ^f	55 ^e	31 ^f	43 ^e		
8	Cl	H	H	44 ^e	67 ^e	43 ^e	76 ^d	51 ^e	94 ^d	30 ^f	55 ^e	31 ^f	43 ^e
9	CH ₂ OH	H	H					10 ^g	90 ^d				
10	OEt	H	H			1 ^g	0 ^g	0 ^g	29 ^f				
11	Me	Me	H			6 ^g	8 ^g	4 ^g	15 ^g				
12	OMe	OMe	H			4 ^g	11 ^g						
13	Cl	Cl	H			52 ^e	76 ^d	20 ^g	62 ^e				
14	H	H	F			15 ^g	34 ^f	82 ^d	98 ^d				
15	H	H	Cl			3 ^g	14 ^g	4 ^g	2 ^g				

^aActivities of 1–3, 6–8, and 10 in inducing HL-60R and MDA-MB-231 apoptosis and growth inhibition were previously reported.¹¹ ^bResults represent the average of triplicates $\pm \leq 10$ (standard deviation). ^cCalculated volumes (cubic angstroms) of X: H, 5.77; F, 10.7; Cl, 19.3; Me, 22.3; CH₂OH, 30.6; OMe, 31.3; OEt, 48.1.⁴⁷ ^dStatistical analysis (probability of difference of the treatment value from that of the nontreated control): $P < 0.001$. ^eStatistical analysis (probability of difference of the treatment value from that of the nontreated control): $P < 0.01$. ^fStatistical analysis (probability of difference of the treatment value from that of the nontreated control): $P < 0.05$. ^gStatistical analysis (probability of difference of the treatment value from that of the nontreated control): $P > 0.05$.

Benzylation of phenols 18 and 20 provided the 3-benzyloxyphenyl bromides 19 and 21 for preparing the respective intermediates 26 and 29. Palladium-catalyzed acrylation of 26 and 29, BBr₃-mediated debenzylation, and treatment with triflic anhydride yielded the ethyl 3-cyano- and 3-carbomethoxy-4-triflyloxybenzoates 28 and 31, respectively. Diisobutylaluminum hydride reduction of 4-bromo-3-methoxybenzocyanide (22) provided benzaldehyde 23. Both 23 and 24 underwent a Wittig olefination to afford the respective 3-methoxy- and 3-nitro-4-bromocinnamate ester intermediates 32 and 33.

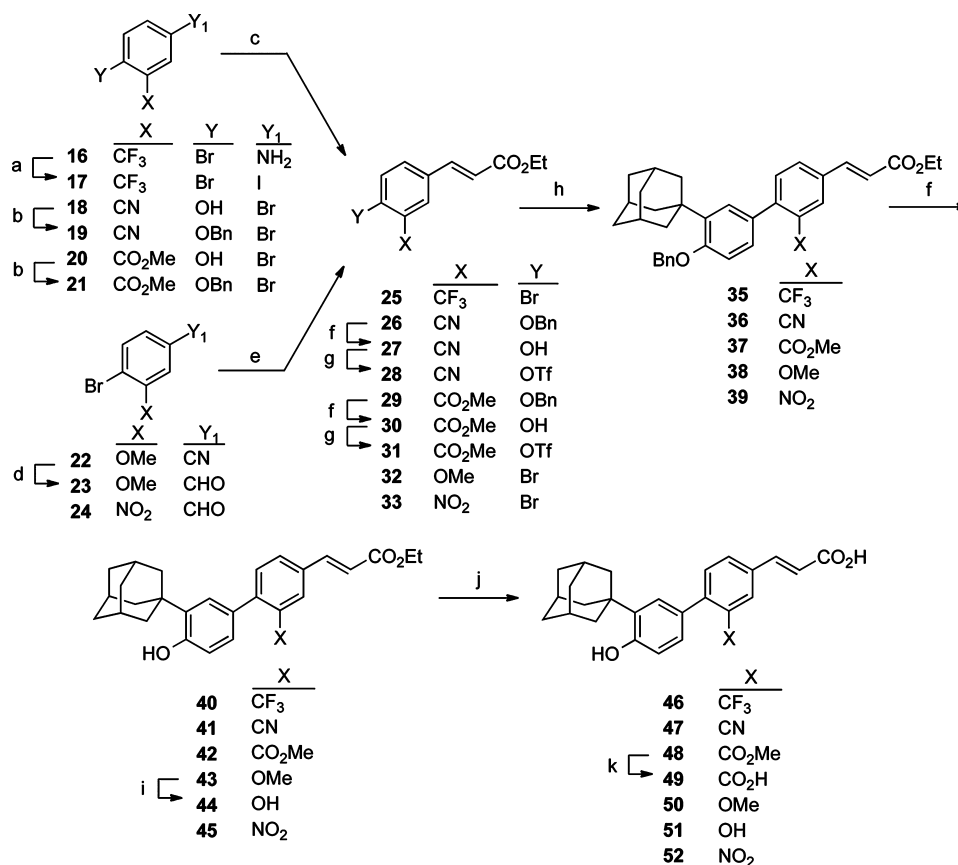
Palladium-catalyzed coupling of aryl bromides 25, 32, and 33 and aryl triflates 28 and 31 with 34 produced the protected 4-arylcinnamates 35, 38, 39, 36, and 37, respectively, which were then debenzylated by using BBr₃. Another BBr₃-mediated cleavage of the 3-methoxy group of 43 gave 3-OH-substituted 44. Base hydrolysis and acidification yielded target cinnamic acids 46–48 and 50–52. The hindered 3-carbomethoxy group of 48 did not hydrolyze at 0–22 °C, which was routinely used for the ethyl ester hydrolysis, but did at 82 °C to afford 3-carboxy-substituted 49 (71%).

The 3-nitrocinnamate 39 was also used to prepare analogues 57, 59, 61, 63, 66, and 69 (Scheme 2). Reduction of the 3-nitro group of 39 using stannous chloride in ethanol provided 3-aminocinnamate 53. Diazotization of 53 under hydrophobic conditions using *tert*-butyl nitrite in the presence of cupric bromide (2 equiv) at 0–22 °C produced the 2,5-dibromocinnamate 55. In contrast, treatment of 53 with *n*-hexyl nitrite in bromoform (34 equiv) at 100 °C afforded the 3-bromocinnamate 54.

Debenzylation of 53–55 produced 56, 60, and 62, respectively, which were hydrolyzed to provide their respective 3-amino-, 3-bromo-, and 2,5-dibromocinnamic acids 57, 61, and 63. The amino group of 56 was diazotized (HNO₂) and treated with sodium azide to produce 3-azidocinnamate 58, which after ester hydrolysis provided 3-azidocinnamic acid 59. Reductive cyclization of 39 by heating (180 °C) with triphenylphosphine in 1,2-dichlorobenzene^{18,19} afforded the regioisomeric carbazoles 64 and 67, which were separated and then deprotected in two steps to give 66 and 69, respectively.

Biological Evaluation. Antiproliferative and Apoptotic Activities. Analogues 46–52, 57, 59, 61, 63, 66, and 69 were compared to the 3-chloro congener (8) for their ability to inhibit proliferation or viability of four human leukemia cell lines (KG-1 AML, OCI-AML2 AML, K562 CML, and MOLT4 T-ALL) and induce KG-1 cell apoptosis (Table 2). These cell lines were selected as representative of the acute myeloid, chronic myeloid, and T-cell acute lymphoblastic types of leukemia having varied resistances to synthetic retinoid 1 from which these analogues were originally derived^{20,21} and to chemotherapeutic agents and a variety of defects that facilitates their proliferation,^{22–39} which are described in the Supporting Information. The KG-1 AML line was also used for comparison with the activities of the first-generation analogues (see Table 1).

The viability of these leukemia lines was determined after treatment for 72 h by measuring changes in their ATP levels using assays for luciferase, for which ATP serves as a cofactor (Table 2). The dose–response curves used to determine their

Scheme 1. Syntheses of 46–52^a

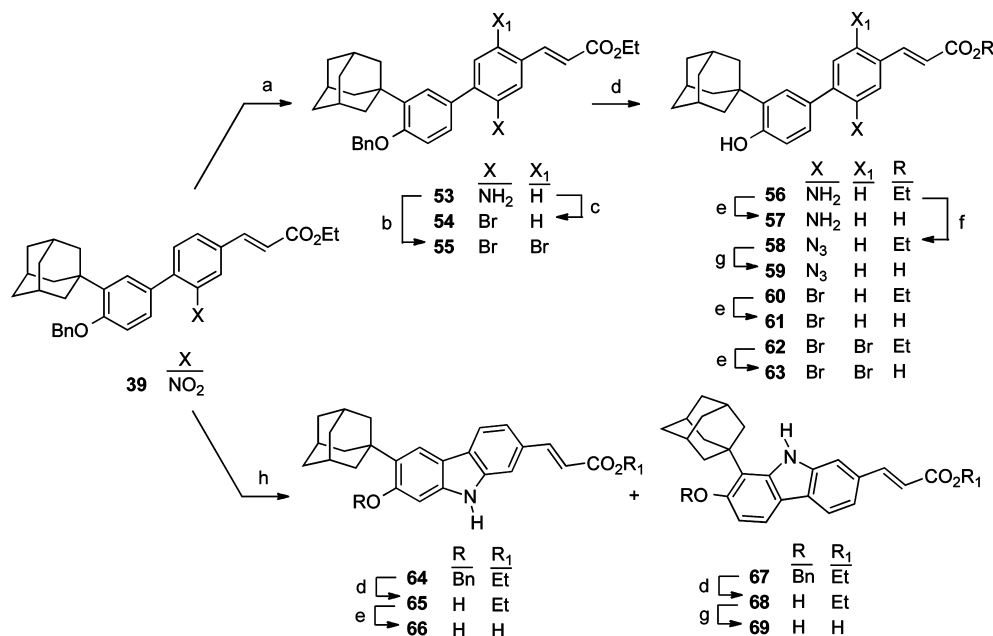
^aReagents and conditions: (a) NaNO₂, H₂SO₄, 0 to 5 °C, KI, room temperature to 100 °C; (b) PhCH₂Br, K₂CO₃, acetone, reflux; (c) ethyl acrylate, Pd(OAc)₂, Et₃N, tri(*o*-tolyl)phosphine, reflux; (d) DIBAL, MePh, -78 °C to room temperature; MeOH, 10% H₂SO₄; (e) (carboxymethylene)-Ph₃P, MePh, reflux; (f) BBr₃, CH₂Cl₂, -78 °C; H₂O; (g) Tf₂O, pyridine, CH₂Cl₂, 0 °C to room temperature; (h) for compounds 35, 38, and 39, 3-(1-adamantyl)-4-benzyloxyphenylboronic acid (34), Pd(PPh₃)₄, DME, 2 M Na₂CO₃, reflux; for compounds 36 and 37, compound 34, Pd(PPh₃)₄, LiCl, DME, 2 M Na₂CO₃, reflux; (i) BBr₃, CH₂Cl₂, -78 °C to room temperature; H₂O; (j) for compounds 46, 48, and 51, aqueous NaOH, MeOH, reflux; H₃O⁺; for compounds 47, 50, and 52, LiOH·H₂O, THF/MeOH/H₂O, room temperature; H₃O⁺; (k) LiOH·H₂O, 5 M NaOH, THF/MeOH/H₂O, room temperature to 82 °C; H₃O⁺.

IC₅₀ values are shown in Figure S1 of the Supporting Information. Analysis of the effects of the analogues on these leukemia lines indicated that both the volume and electron density of the substituent at position 3 on the cinnamic ring impacted antiproliferative activities. In analogues that induced the highest levels of KG-1 cell growth inhibition and apoptosis, a variety of polar substituents were tolerated, including 3-Cl, CN, OMe, NO₂, NH₂, N₃, and Br. Of these, the 3-OMe and Br groups of 50 and 61, respectively, provided the most potent KG-1 growth inhibitory activity at 1.0 and 5.0 μM, which approximated that of 8 having a 3-Cl group, whereas all six groups exhibited similar potencies in inducing KG-1 apoptosis. In contrast, 48 and 51 with 3-CO₂Me and 3-OH groups, respectively, were approximately half as potent at 5.0 μM in inducing apoptosis. Analogues 46 and 49 with 3-CF₃ and 3-CO₂H groups, respectively, were essentially inactive. These substituent effects were observed to track with analogue potencies in inhibiting K562, OCI-AML2, and MOLT4 cell viability. In terms of IC₅₀ values, OCI-AML2 AML and MOLT4 T-ALL cells were more sensitive (approximately 3–4-fold) to the analogues than K562 CML cells. Analogues that inhibited viability could be sorted into two groups on the basis of their IC₅₀ values with those having 3-Cl, CN, OH, NO₂, and NH₂ groups being approximately twice as potent as those with

the 3-OMe, N₃, and Br groups. An anomaly to these trends was the 3-CF₃ group of 46. At 5.0 μM, 46 was unable to induce KG-1 cell apoptosis after 48 h but did inhibit OCI-AML2 and MOLT4 viability by 50% at 3.8 and 3.9 μM, respectively, at 72 h, whereas at 5.0 μM, K562 cell viability was inhibited by only 25%. The second anomaly was the lack of activity of 49 having the 3-CO₂H group. The deprotonation of this group at physiologic pH may have impeded the cellular uptake of 49.

Introducing a second group at position 5 of the cinnamic ring led to a further decrease in apoptotic activity in the 3,5-dimethyl, dimethoxy, and dichloro analogues (11–13, respectively) compared to their respective monosubstituted analogues (7, 50, 8, and 61). In contrast to the growth inhibitory and apoptotic activities provided by the 3-amino analogue 57, its planar analogues 66 and 69 having their diaryl rings linked through an *o*-NH group had very low or no activity against the four leukemia cell lines.

Introducing a second bromo group at position 6 of the cinnamic ring of the 3-bromocinnamic acid 61 produced 63 with substantially lower KG-1 apoptosis-inducing activity. At 1.0 μM, 63 was inactive and its IC₅₀ values for inhibiting leukemia cell viability ranged from 1.4 to 4.2 μM. This result is in agreement with the observation that shifting the chloro group to position 2 of the cinnamyl ring in 15 led to a loss of

Scheme 2. Syntheses of 57, 59, 61, 63, 66, and 69^a

^aReagents and conditions: (a) SnCl₂·H₂O, EtOH, 80 °C; (b) CuBr₂, *tert*-butyl nitrite, MeCN, 0 °C to room temperature; (c) *n*-hexyl nitrite, CHBr₃, 100 °C; (d) BBr₃, CH₂Cl₂, -78 °C; H₂O; (e) LiOH·H₂O, THF/MeOH/H₂O, room temperature; H₃O⁺; (f) 2 M H₂SO₄, NaNO₂, dioxane, -10 °C; NaN₃, H₂O, -10 °C; (g) 25% NaOH, EtOH/Et₂O (2:1) (59) or EtOH (69), room temperature; H₃O⁺; (h) PPh₃, 1,2-dichlorobenzene, 180 °C.

MDA-MB-231 growth inhibition and HL-60R AML cell apoptosis-inducing activities, whereas its replacement with the smaller fluorine in 14 retained HL-60R apoptotic activity but reduced the level of MDA-MB-231 growth inhibition compared to that of 6, which had a hydrogen at position 3. In summary, of the new analogues, those having 3-CN, OH, NO₂, and NH₂ groups (47, 51, 52, and 57, respectively) most potently inhibited leukemia cell viability with IC₅₀ values comparable to those of 3-Cl-substituted 8. These four groups have unpaired electrons that could function as H-bond acceptors. Of these, the hydroxyl and amino groups could also function as H-bond donors. The 3-Cl group of 8 could interact with electron-donating atoms (O of T55 and S of C56)⁴⁰ or perhaps have van der Waals interactions with the methyl group of T55.⁴¹

SAR Analysis. The impact of the size of the substituent at position 3 on apoptotic activity was demonstrated previously by the inability of the 3-(3-acetamidopropoxy) analogue (3-A-AHPC, 5) to induce apoptosis; on the other hand, the 3-Cl analogue (8) was active.¹¹ A component SAR analysis (Table S2 and Figure S2 of the Supporting Information) using 11 analogues was undertaken to investigate the impact of the volume of the substituent at position 3 on K562, OCI-AML2, and MOLT-4 leukemia cell viability as determined by the decrease in ATP levels (Table 2). This analysis excluded inactive 49 (X = CO₂H), inactive planar 66 and 69, and 63 with a 3,6-dibrominated cinnamyl ring to provide a series of active and similar compounds. Despite the fact that a downstream event (loss of the mitochondrial generation of ATP) was measured in cells that also were required to take up the analogues through the cell membrane, correlations were obtained in the log-log plots of the volume of the substituent at position 3 versus IC₅₀ values for the three leukemia cell lines. The less active compounds had substituents at position 3 with larger volumes (Figure S2B of the Supporting Information). Thus, 46 with a 3-CF₃ group (37 Å³) and 48 with a 3-CO₂Me

group (50.3 Å³) were the least active, whereas 52 with a 3-NO₂ group (29 Å³) and 59 with a 3-N₃ group (31 Å³) were active. This trend was evident upon comparison of similar substituents. For example, 8 with a smaller 3-Cl group (19 Å³) was 1.9–3.0-fold more active than 61 with a 3-Br group (24 Å³), and 47 with a 3-CN group (23 Å³) was 2.4–4.5-fold more active than 59 with a 3-N₃ group (30.7 Å³).

Next, the combined impact of the volume of the substituent at position 3 and H-bond acceptor and donor capacity on the inhibition of MOLT4 cell viability was examined using comparative molecular field analysis (CoMFA) (Figure 2). The resulting partial contour map shows that the favored steric and positively charged fields were asymmetric and that the favored negatively charged field was symmetric (Figure 2A). The large red contour map suggests that an H-bond acceptor would have a wider role in interacting with a SHP pocket residue to support the higher activities observed for analogues 47, 51, 52, and 57. Similar partial contour maps were obtained from analyses of the results from the treatment of K562 and OCI-AML2 cells. In Figure 2B are shown plots of the actual and predicted logarithms of the IC₅₀ values for viability inhibition of the three cell lines obtained from the CoMFA studies that suggest robust correlations. The data used to construct the three maps are summarized in Tables S2 and S3 of the Supporting Information. These trends continued when comparing the physical properties of the substituents at position 3 of the 11 analogues with their KG-1 apoptosis-inducing activities.

The most active analogues (8, 47, 51, 52, and 57) together with much less active analogue 46 were also evaluated for their effects on MMTV-Wnt1 murine mammary cancer stem cell proliferation. Their dose-response curves are shown in Figure 3. On the basis of the IC₅₀ values (Table 2) obtained from these curves, analogues with 3-Cl and NH₂ groups (8 and 57, respectively) had comparable activity and were more potent

Table 2. Effects of a Substituent at Position 3 of the AHPC Scaffold on KG-1 AML Cell Growth Inhibition and Apoptosis Induction and Inhibition of Leukemia Cell (K562, OCI-AML2, and MOLT4) and Mammary Cancer Stem Cell Viability

compound	X ^d	X ₁	KG-1AML at 48 h				leukemia cell viability at 72 h			MMTV-Wnt1 murine mammary stem cell viability at 72 h IC ₅₀ (μM) ^e
			growth inhibition (%) ^a		apoptosis (%) ^a		IC ₅₀ (μM), (% at 5 μM) ^b			
			1.0 μM	5.0 μM	1.0 μM	5.0 μM	K562 AML	OCI-AML2	MOLT4 T-ALL	
8	Cl	H	44 ^e	67 ^e	30 ^f	55 ^e	0.54 (12±0.7)	0.17 (2.0±0.1)	0.16 (4.8±0.2)	0.047 ±0.002
46	CF ₃	H	8 ^f	14 ^f	4 ^f	4 ^f	>5 (75±2.3)	3.75 (27±2.7)	3.91 (26±1.2)	2.86 ±0.35 ⁱ
47	CN	H	39 ^e	51 ^e	39 ^e	51 ^e	0.68 (10±0.4)	0.10 (2.0±0.0)	0.14 (3.9±0.2)	0.072 ±0.004 ⁱ
48	CO ₂ Me	H	6 ^f	29 ^g	1 ^f	22 ^g	5.6 ^h (55±1.6)	0.87 (2.2±0.1)	1.02 (7.2±0.2)	nd ^m
49	CO ₂ H	H	7 ^f	16 ^f	4 ^f	7 ^f	>5 (94±3.0)	>5 (109±11)	>5 (107 ±4.6)	nd
50	OMe	H	45 ^e	64 ^e	31 ^g	51 ^e	1.30 (21±1.1)	0.29 (3.0±0.1)	0.33 (5.7±0.2)	nd
51	OH	H	23 ^g	39 ^e	18 ^f	28 ^g	0.67 (17±0.7)	0.14 (2.1±0.1)	0.16 (6.7±0.4)	0.063 ±0.007 ^j
52	NO ₂	H	40 ^e	51 ^e	34 ^g	48 ^e	0.69 (14±0.5)	0.13 (2.0±0.0)	0.16 (5.1±0.1)	0.061 ±0.003 ^k
57	NH ₂	H	39 ^e	49 ^e	37 ^g	52 ^e	0.68 (22±0.8)	0.15 (2.9±0.2)	0.17 (8.1±0.4)	0.049 ±0.003 ^l
59	N ₃	H	37 ^g	51 ^e	27 ^g	48 ^e	1.63 (26±1.2)	0.45 (4.0±0.1)	0.46 (6.8±0.2)	nd
61	Br	H	36 ^g	58 ^e	37 ^g	47 ^f	1.60 (20±1.0)	0.32 (2.2±0.0)	0.35 (6.0±0.3)	nd
63	Br	Br	6 ^f	48 ^e	1 ^f	22 ^f	4.20 (44±9.9)	1.36 (2.0±0.1)	1.65 (0.1±0.2)	nd
66			18 ^f	30 ^g	5 ^f	10 ^f	>5 (82±8.3)	>5 (103 ±6.7)	>5 (86±1.8)	nd
69			10 ^f	17 ^f	4 ^f	7 ^f	>5 (75±5.4)	>5 (89±2.7)	>5 (64±2.9)	nd

^aResults represent the means of triplicates ± 10 [standard deviation (SD)]. ^bLeukemia cell lines treated with 0, 0.1, 0.25, 0.5, 1.0, 2.5, and 5.0 μM compound. IC₅₀ values were determined from the dose–response curves shown in Figure S1 of the Supporting Information using data representing means of quadruplicate trials ± SD (K562, ≤10; OCI-AML2, ≤11; MOLT4, ≤10), as was the determination of viability (percent at 5 μM). ^cCells treated with 0, 0.01, 0.03, 0.1, 0.3, 1.0, and 3.0 μM compound. IC₅₀ values determined graphically from each of triplicate dose–response curves are represented as means of triplicates ± SD. ^dCalculated volume (cubic angstroms) of X: Cl, 19.3; CF₃, 37.1; CN, 22.6; CO₂Me, 50.3; CO₂H, 32.8; OMe, 31.3; OH, 13.8; NO₂, 29.1; NH₂, 17.1; N₃, 30.7; Br, 23.7.⁴⁷ ^eStatistical analysis (probability of difference of the treatment value from that of the nontreated control): *P* < 0.05. ^fStatistical analysis (probability of difference of the treatment value from that of the nontreated control): *P* < 0.05. ^gStatistical analysis (probability of difference of the treatment value from that of the nontreated control): *P* < 0.05. ^hExtrapolated value. ⁱStatistical analysis (probability of difference of the analogue IC₅₀ value from that of 8): *P* < 0.001. ^jStatistical analysis (probability of difference of the analogue IC₅₀ value from that of 8): *P* < 0.01. ^kStatistical analysis (probability of difference of the analogue IC₅₀ value from that of 8): *P* < 0.005. ^lStatistical analysis (probability of difference of the analogue IC₅₀ value from that of 8): *P* > 0.1. ^mnd, not determined.

than analogues with 3-CN, OH, and NO₂ groups (47, 51, and 52, respectively). Compound 46 inhibited MMTV-Wnt1 proliferation with an IC₅₀ value of 2.37 μM, which was more than 50-fold higher than that determined for 8. The IC₅₀ values of analogues in the MMTV-Wnt1 murine mammary stem cell assay were much lower than those obtained using the leukemia cell lines as would be expected for cells growing in media without serum.

Binding to SHP. As one of the active analogues listed in Table 2, 47 (X = CN) was selected to illustrate how interaction with SHP protein could have roles in leukemia cell apoptosis induction and inhibition of cell viability. SHP has thus far defied

crystallization and structure determination. In our hands, the recombinant wild-type human protein proved to be too labile for determining binding using isothermal titration calorimetry, and therefore, we resorted to low-temperature, high-field NMR spectrometry. Binding of 47 to SHP (Figure 4A) was demonstrated in comparison with 8 (X = Cl) (Figure 4B) as a positive SHP-binding control. Compound 8 was previously shown to bind to SHP in a competitive binding assay with [5,5-³H₂]AHPN.¹ The 6.3–7.9 ppm region of the NMR spectra of the compounds was selected for comparison because ligand proton signals in that region were not obscured by extraneous proton signals from water, tris(hydroxymethyl)aminomethane in

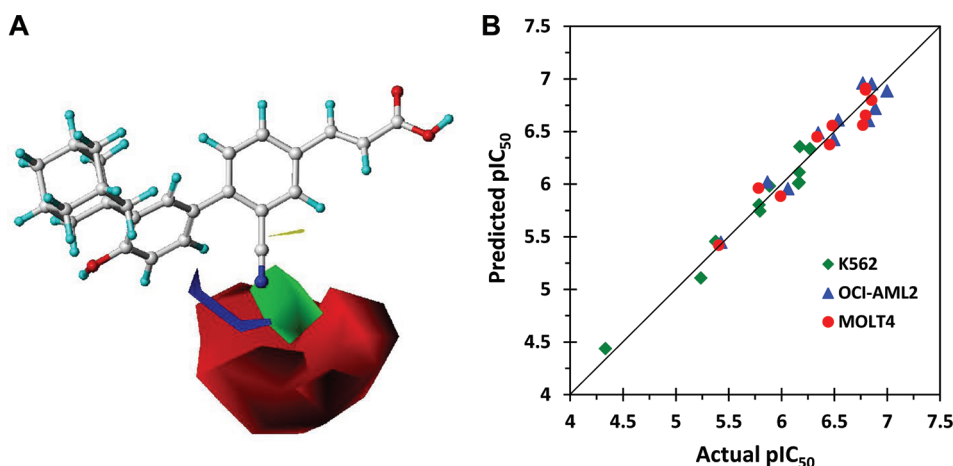


Figure 2. CoMFA of replacement of the 3-chloro group of **8** on leukemia cell viability. (A) Partial CoMFA contour maps (StDev*Coeff) for steric and electrostatic fields about the substituent at position 3 based on MOLT4 IC_{50} viability data with analogue **47** displayed as a visual reference. Favored steric contributions are colored green and disfavored steric contributions yellow; the blue contour indicates regions where positive charges are favored and red regions where negative charge is favored. (B) Plot of predicted vs actual pIC_{50} values of inhibition of leukemia cell viability by **8**, **46–48**, **50–52**, **57**, **59**, **61**, and **62** for K562 (green diamonds), OCI-AML2 (blue triangles), and MOLT4 (red dots) leukemia cell lines determined by CoMFA.

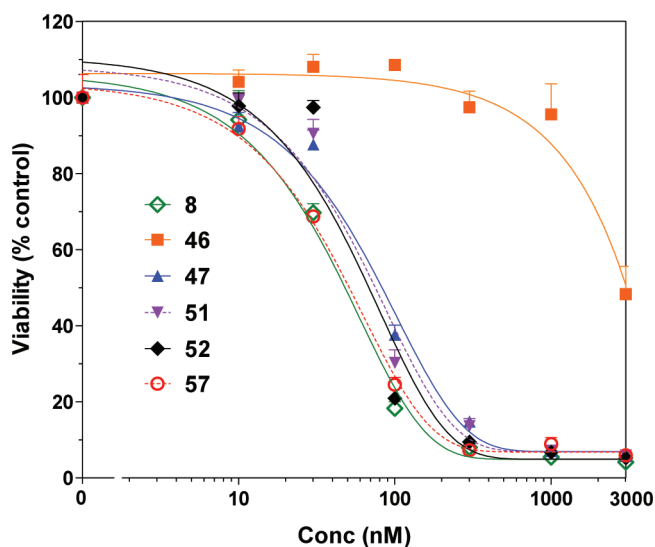


Figure 3. Effects of **8**, **46**, **47**, **51**, **52**, and **57** on MMTV-Wnt1 mammary cancer stem cell viability as measured by DAPI staining and cell counting. Cells were treated with each analogue at the indicated concentrations or with vehicle alone (Me_2SO control) for 72 h before the viability of treated cells relative to vehicle-treated control was determined. Results represent the means of triplicates \pm the standard deviation.

Tris buffer, reduced glutathione, and DMSO, which were present at higher concentrations. The lower scans in panels A and B of Figure 4 show that the peak heights of the six aromatic and two olefinic protons in this region of the spectra of both **47** and **8** were decreased and broadened in the presence of SHP, thereby indicating their interaction with the protein. In contrast, proton signals for inactive analogue **46** ($X = CF_3$) were not depressed by the addition of SHP (Figure 4C), thereby indicating the absence or only a very weak interaction of **46** with the protein.

Computational Studies. Docking to the SHP Model.

To discern how the substituent at position 3 impacted SHP in its inhibition of cell viability, docking studies (Figure 5) were conducted using the three-dimensional model of SHP derived

from the structure of the homologous USP LBD by the Pelliccaria group.⁶ In the model, SHP helix H12 assumed the canonical agonist position to form an AF-2 surface with H3 and H4. This model also has a putative ligand-binding pocket (LBP) to which the USP phospholipid ligand and analogues **1**, **3**, and **8** had been successfully docked.^{6,13} The docking poses for **1**, **3**, and **8** were highly similar and suggested potential stabilizing interactions with the following LBP residues: T55 and C56 (H3), F96, L97, and L100 (H5), P139, A145, and W148 (H7), L231 and L235 (H11), and R238 and I240 (H11–H12 loop).¹³ Formation of ionic and/or H-bonding interactions between an analogue carboxylate group and the R238 guanidinium group and a nonconventional H– π bond between an analogue phenolic hydroxyl group and the F97 phenyl ring were regarded as the most important polar interactions for stabilization.

The docked poses of the current analogues substituted at position 3 were compared with that of **8** (Figure 5A). Active analogues such as **47** ($X = CN$) and **52** ($X = NO_2$) assumed docking poses similar to that of **8**. The respective distances between their carboxylate carbon atoms and the H11 R238 guanidinium carbon were measured as 4.3 and 4.1 Å, respectively, compared to a value of 3.8 Å for **8**. These distances suggest that their carboxylate groups would contribute H-bond and/or ionic interactions with the R238 guanidinium group to stabilize binding. On the basis of position and distance, the 4'-OH groups of **47** and **52**, like that of **8**, could form H– π bonds with the π -electron cloud of the H5 F96 phenyl ring to enhance analogue–LBP interaction.^{13,42} The respective distances between their OH oxygens and the F96 phenyl ring center were 3.0 and 2.8 Å compared to 3.0 Å for **8**. van der Waals interactions between their 3'-(1-Ad) groups and the surrounding LBP W148, L97, and L100 side chains could also occur to further stabilize binding. The shortest distances measured between the 3'-(1-Ad) group carbons of **47** and **52** and the W148 indole ring carbons were 3.6 and 3.3 Å, respectively, compared to 3.9 Å for **8**. Similarly, the shortest distances measured from their 3'-(1-Ad) group carbons to one of the L97 methyl carbons were 3.7 and 4.1 Å, respectively, compared to 3.9 Å for **8**, and those to one of the L100 methyl carbons were 3.8 and 4.2 Å, respectively, compared to 3.6 Å for **8**.

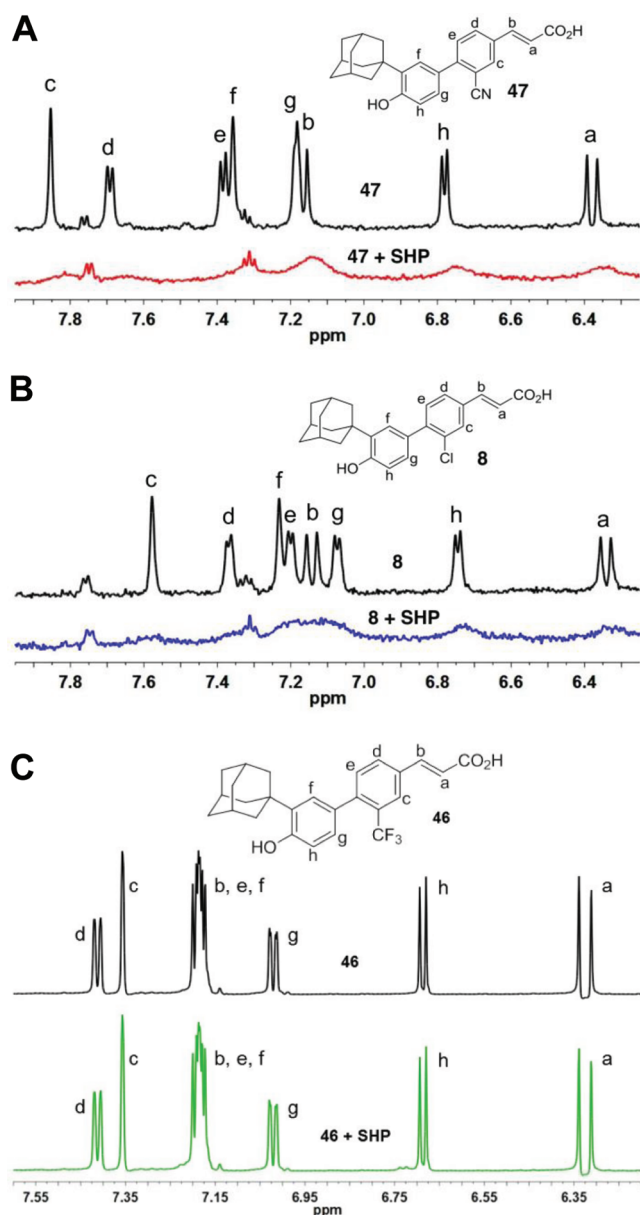


Figure 4. ^1H NMR spectra indicate that apoptosis-inducing 3-cyanocinnamic acid **47** binds to SHP, whereas inactive 3-(trifluoromethyl)cinnamic acid **46** does not. The low-field regions of one-dimensional ^1H NMR spectra of **47**, **46**, and **8** alone and in the presence of recombinant human SHP are shown. Spectra were recorded at 11 °C on (A) **47** (100 μM), (B) **8** (100 μM), and (C) **46** (200 μM) in the absence (top spectra) and presence (bottom spectra) of 0.5 (A and B) and 1.0 μM SHP protein (C). Note that small peaks at 7.3 and 7.75 ppm in panels A and B represent an impurity in the D_2O (see Figure S4 of the Supporting Information). The spectrum in panel C was that of a sample containing D_2O from another source.

Prior docking using **8** suggested a potential stabilizing interaction could occur between its 3-Cl group and the H3 C56 side chain because of formation of a $\text{Cl}\cdots\text{H}-\text{S}$ bond (4.2 Å $\text{Cl}-\text{S}$ distance).¹³ The measured distances of 3.7 Å from the 3-CN nitrogen of **47** to the C56 sulfur and 4.3 Å from a 3- NO_2 oxygen of **52** to the C56 sulfur suggest that the 3-CN and 3- NO_2 groups could form similar $\text{N}\cdots\text{H}-\text{S}$ and $\text{O}\cdots\text{H}-\text{S}$ H-bonding interactions.⁴³ The docked poses of **47** and **52** also suggest that their 3-CN and 3- NO_2 groups, respectively, could contribute to ligand stabilization by forming hydrogen bonds with the T55 OH group,

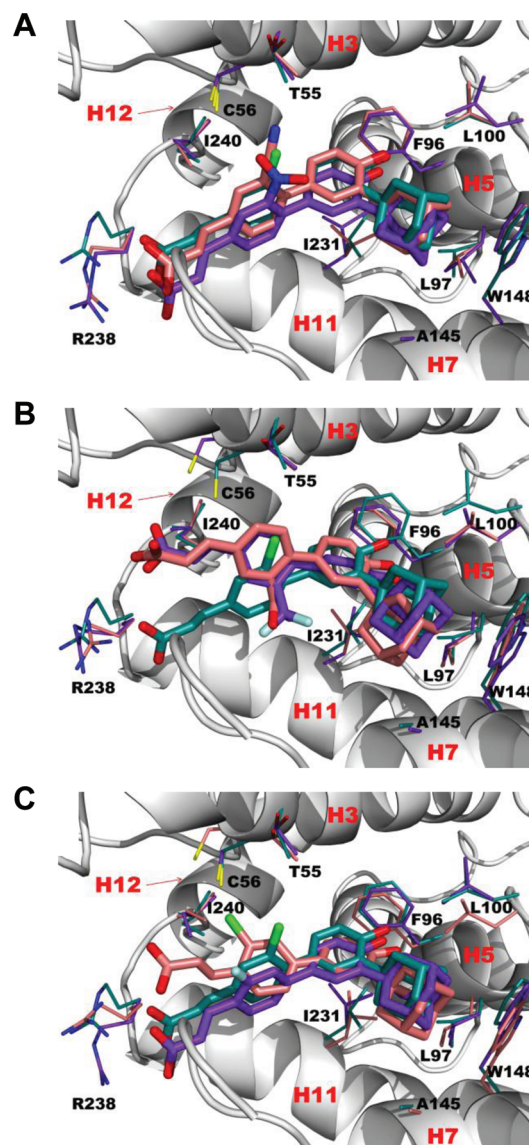


Figure 5. Poses assumed by **8**, **14**, **15**, **46**, **47**, **49**, and **52** upon docking to the ultraspiracle ligand-binding domain-derived model of small heterodimer partner (SHP). (A) Overlap of docking poses for **8**, **47**, and **52** in stick format with LBP residues in line format. C atoms of **8**, **47**, and **52** and those of their corresponding pocket residues are colored cyan, orange, and magenta, respectively, with other atoms colored as follows: Cl, green; F, light blue; N, blue; O, red; S, yellow. (B) Overlap of docking poses for **8**, **46**, and **49** shown in stick format with LBP residues in line format. C atoms of **8**, **46**, and **49** and those of their corresponding pocket residues are colored cyan, magenta, and orange, respectively, with other atoms colored as in panel A. (C) Overlap of docking poses for **8**, **14**, and **15** shown in stick format with conformations of SHP ligand-binding pocket (LBP) residues shown in line format. C atoms of **8**, **14**, and **15** and those of their corresponding pocket residues are colored cyan, magenta, and orange, respectively, with other atoms colored as in panel A. The residue numbering is that for the human SHP protein sequence. Docking studies were performed using BioMed Cache version 6.2 with flexible ligands and protein side chains. **8**, **14**, **47**, and **52** were classified as active compounds, whereas analogues **15**, **46**, and **49** were inactive or less active in terms of growth inhibition, loss of viability, or apoptosis induction.

just as that of **8** suggests its 3-Cl could form a similar bond with the OH group, while the two aromatic rings of these analogues could make hydrophobic contacts with the side chains of L231, L235, and I240.

Analogues without or with very weak activity such as **46** ($X = \text{CF}_3$) and **49** ($X = \text{CO}_2\text{H}$) assumed docking poses that differed from that of 3-Cl-AHPC (Figure 5B). Their carboxylates were farther from the R238 guanidinium group than that of **8**, and their substituents at position 3 were oriented toward hydrophobic LBP residues rather than T55 and C56, which is shown in the overlap of their docking poses in the SHP LBP. The measured distances from the carboxylate carbons of **46** and **49** to the R238 guanidinium carbon of 5.8 and 5.1 Å, respectively, suggest only weak or no H-bond or salt bridge interactions would occur in contrast to those possible for the carboxylate of **8**. Their 3- CF_3 and 3- CO_2H groups would occupy a side pocket between the H7 P141 and H11 L235 side chains, where their respective fluorine and oxygen atoms would be unable to function as H-bond acceptors. These poses also suggest that their 4'-OH groups, which are farther from the F96 phenyl ring (OH O—phenyl center distances of 4.0 and 4.1 Å, respectively) than that of **8** (3.0 Å), would contribute weaker or no stabilizing H- π bond interactions. Although the poses do suggest that the 3'-(1-Ad) groups of **46** and **49** could interact with the hydrophobic side chains of L97, L100, A145, and W148 (e.g., the shortest distance to the W148 indole ring was 3.4 Å compared to 3.9 Å for **8**), their contributions by being weaker would contribute far less to binding stabilization, thereby limiting the residence time of the analogue in the LBP in agreement with their lack of activity.

Analogues with substituents at position 2 such as **14** (2-F) and **15** (2-Cl) were also docked and compared with **8** (2-H) (Figure 5C). Active **14** with the smaller F group at position 2 had a pose similar to that of **8**. In contrast, inactive **15** with the larger 2-Cl group had a pose in which its cinnamic moiety was farther from H11 and closer to H12 than that of **8**. As a result, the distance (4.7 Å) between the carboxylate carbon of **15** and the R238 guanidinium carbon, by being longer, suggests that any H-bond or ionic interactions with the R238 guanidinium group would be weaker. The short distance (2.46 Å) between the 2-Cl atom and I240 side chain methyl carbon suggests a potential clash that would prevent robust interaction with the pocket. Thus, while the inactive analogues could be docked into the SHP LBP, their poses suggest that any polar interactions between the analogue and LBP residues required for stabilizing binding would be absent or weak.

DISCUSSION

Our results indicate that the leukemia cell apoptosis-inducing and viability-inhibiting activities of 3-substituted analogues of **8** would be retained if the substituents had some electron-donating (H-bond-accepting) capacity and restricted volumes.

Recently, Pelliccari, Wang, and co-workers conducted an elegant series of computational and mutagenesis studies to examine the SHP LBP. Several models of the SHP protein were constructed on the basis of its homology to the phospholipid-complexed USP LBD, docosahexaenoic acid and oleic acid-complexed RXR α LBD, and DAX-1 using their reported crystal structures.⁷ These models displayed either the canonical NR LBP such as those found in the ligand-bound PPARs, RARs, RXRs, TRs, and VDR or another pocket that they termed “allosteric” such as that found in NRs bound to charged phospholipids such as USP, SF-1, and LRH-1. Both allosteric and canonical models featured an L-shaped LBP; however, docking studies revealed that **8** occupied different arms of the L with its adamantyl group residing at the arm juncture so that its carboxylate could interact with either Gln140 (allosteric USP-

derived model) or R34 (canonical DAX-1-derived model), whereas the antagonist **5**¹¹ assumed a pose in which its carboxylate interacted with R238 (USP-derived model). Molecular dynamics using the USP-derived model suggested that H-bond and/or ionic stabilizing interactions were favored between the **8** carboxylate and SHP R238 (80%) followed by Q140 (18%) and R138 (17%) and that SHP NR boxes 1 and 3 were stabilized by **8**, whereas NR box 2 and the H12 agonist position were destabilized.

Mutational analysis indicated that unlike wild-type SHP, the double mutant L5-6 R138D/H11 R238D, in which reversal of side chain charge would not support interaction with a ligand carboxyl group, and the H3 F96A point mutant, which by lacking the phenyl ring was incapable of stabilizing the ligand hydroxyl group, were unable to block HNF4 α transactivation of its site on the ApoCIII promoter–Luc reporter construct, thereby suggesting that R138, R238, and F96 played roles in mediating SHP repressor activity. Moreover, F96A and R138D/R238D mutants prevented SHP from inhibiting basal HNF4 α activation by 44%, whereas the W148A, R238A, R138A, W92A, R34A, and R34Q/Q134R mutants did not have a similar effect. Although SHP antagonist **5** [$X = \text{O}-(\text{CH}_2)_3\text{NHAc}$] did dock into the LBP “canonical” arm of the DAX-1-derived model to suggest that its pharmacophoric elements (carboxylate and hydroxyl) could interact with other LBP residues, their mutation to alanine did not affect the ability of SHP to repress HNF4 α transactivation and so did not support this canonical model. These mutational studies support our use of the USP LBD-derived “allosteric model” for ligand design. In this model, docking places the carboxylate of **8** at the pocket entrance, as do the charged termini of phospholipids bound to USP, SF-1, and LRH-1. Much remains to be learned about SHP, including the impact of ligands on NR box motif stabilization and the actual geometry of the LBP in the presence of a ligand, which highlight the necessity of determining the actual structure of SHP.

Conclusion. The results indicate that leukemia cell apoptotic activity and inhibition of cell viability are retained in analogues of **8** as long as their substituents at position 3 had some electron donor (H-bond-accepting) capacity and restricted volume.

EXPERIMENTAL SECTION

Chemistry. General Methods. Chemicals and solvents from commercial sources were used without further purification. 3-(1-Adamantyl)-4-benzyloxyphenylboronic acid (**34**) was synthesized using our reported procedure.¹⁴ Abbreviations for solvents and reagents are as follows: BnBr, benzyl bromide; DIBAL, diisobutylaluminum hydride; DME, 1,2-dimethoxyethane; Tf₂O, trifluoromethanesulfonic anhydride. Experimental procedures were not optimized. Anhydrous and/or oxygen-sensitive reactions were conducted under argon gas. Reactions were monitored by thin-layer chromatography on silica gel (mesh size 60, F₂₅₄) with visualization under UV light. Unless specified, the standard workup involved washing the organic extract with water and brine and drying over Na₂SO₄ followed by concentration at reduced pressure. Chromatography refers to flash column chromatography on silica gel (Merck 60, 230–400 mesh). Melting points of samples were determined in capillaries using a Mel-Temp II apparatus and are uncorrected. Infrared spectra were obtained on powdered or liquid samples using an FT-IR Mason satellite spectrophotometer. ¹H NMR spectra were recorded on a 300 MHz Varian Unity Inova spectrometer or an ECS 400 MHz Jeol spectrometer, and shift values are expressed in parts per million (δ) relative to CHCl₃ as the internal standard. Unless mentioned, NMR samples were dissolved in ²HCCl₃. High-resolution mass spectra were recorded on an Agilent ESI-TOF mass spectrometer at The Scripps Research Institute (La Jolla, CA). A Shimadzu HPLC system was used to analyze the purity of target

molecules (Table S4 of the Supporting Information). General synthetic methods are described first and designated by letters. Then compound syntheses and characterizations are listed numerically. The purity of compounds used in the biological assays was >95% as determined by reversed-phase HPLC (Table S4 of the Supporting Information lists actual purities). The purity of **8** was 98% as determined by reversed-phase HPLC analysis. The SHP residue numbering used in the model and protein followed that given for human SHP protein (identifier Q15466) in the UniProtKB protein database; thus, SHP model residue numbers⁶ were increased by 13.

General Method A: Protection of Phenols 18 and 20 as Benzyl Ethers 19 and 21, Respectively. To a solution of the phenol (1 mmol) in acetone (3 mL) were added K_2CO_3 (1.13 mmol) and $BnBr$ (1.05 mmol). This mixture was stirred at reflux temperature under argon. After removal of acetone at reduced pressure, 1 N HCl was added. This mixture was extracted (EtOAc). The residue obtained upon concentration of the extract was chromatographed to give the benzyl ether.

General Method B: Coupling of Ethyl Acrylate with Aryl Halides 17, 19, and 21 To Afford Ethyl Cinnamates 25, 26, and 29, Respectively. A solution of the aryl halide (1.0 mmol), ethyl acrylate (1.3 mmol), palladium(II) acetate (0.015 mmol), and tri(*o*-tolyl)-phosphine (0.04 mmol) in triethylamine (1.1 mL) was stirred while being heated and then cooled to room temperature, and the reaction was quenched with 1 N HCl. The resulting suspension was extracted (EtOAc). The extract was washed (brine) and dried. After solvent removal at reduced pressure, the residue was purified on silica gel to give the cinnamate ester.

General Method C: Ethyl Cinnamates 32 and 33 by Wittig Reaction of (Carbomethoxymethylene)triphenylphosphorane with Aryl Aldehydes 23 and 24, Respectively. A solution of aryl aldehyde (1.0 mmol) and (carbomethoxymethylene)triphenylphosphorane (1.15 mmol) in PhMe (2.9 mL) was heated at reflux and then cooled to room temperature. After solvent removal at reduced pressure, the residue was chromatographed to give the cinnamate.

General Method D: Debromination of 26, 29, 35–39, 53–55, 64, and 67 Using Boron Tribromide. To a stirred solution of the benzyl ether (1.0 mmol) in CH_2Cl_2 (8 mL) at $-78^\circ C$ under argon was slowly added 1.0 M boron tribromide (3.0 mmol) in CH_2Cl_2 (3.0 mL). The mixture was stirred at $-78^\circ C$ for 2 h, the reaction quenched with water (15 mL), and the mixture extracted (EtOAc). The extract was washed (brine) and dried. After solvent removal at reduced pressure, flash chromatography of the residue yielded the phenol.

General Method E: Conversion of Phenols 27 and 30 to Triflates 28 and 31, Respectively. To a stirred solution of the phenol (1.0 mmol) and pyridine (redistilled from KOH, 2.25 mmol) in CH_2Cl_2 (2.5 mL) under argon at $0^\circ C$ was slowly added Tf_2O (1.35 mmol). The resulting solution was allowed to warm to room temperature while being stirred, the reaction quenched with 1 N HCl, and the mixture extracted (CH_2Cl_2). The extract was washed (brine), dried, and concentrated at reduced pressure. The residue was purified by chromatography to afford the triflate.

General Method F: Diaryl Coupling of 3-(1-Adamantyl)-4-benzyloxyphenylboronic Acid (34) with Aryl Halides 25, 32, and 33. To a solution of **34** (1.2 mmol) and aryl halide (1.0 mmol) in degassed DME (6.7 mL) were added tetrakis(triphenylphosphine) palladium (0.12 mmol) and 2 M Na_2CO_3 (degassed, 1.3 mL). The reaction mixture was heated at reflux, cooled to room temperature, diluted with EtOAc, washed (H_2O and brine), and dried. After solvent removal at reduced pressure, flash chromatography on silica gel yielded the coupling product.

General Method G: Coupling of Aryl Boronic Acid 34 to Aryl Triflates 28 and 31. To a stirred solution of **34** (1.17 mmol) and the aryl triflate (1.0 mmol) in degassed DME (8 mL) were added LiCl (2.6 mmol), tetrakis(triphenylphosphine)palladium (0.12 mmol), and 2 M Na_2CO_3 (degassed, 1.2 mL). The reaction mixture was heated at reflux, cooled to room temperature, then diluted with EtOAc, washed (H_2O and brine), and dried. After concentration of the organic layer at reduced pressure, flash chromatography on silica gel yielded the diaryl coupling product.

General Method H: Hydrolysis of Ethyl Cinnamates 40, 42, and 44 to Cinnamic Acids 46, 48, and 51, Respectively, Using Aqueous Sodium Hydroxide. To a stirred solution of the cinnamate (1 mmol) in MeOH (10 mL) was added 5 M aqueous NaOH (5 mmol). This mixture was heated at reflux under argon, cooled to room temperature, acidified with 2 N HCl, and extracted (EtOAc). The extract was washed (brine) and dried. The yellow solid residue obtained by concentration was chromatographed or washed (hexane and CH_2Cl_2 or $CHCl_3$) to afford the cinnamic acid.

General Method I: Hydrolysis of Cinnamates 41, 43, 45, and 65 to Cinnamic Acids 47, 50, 52, and 66, Respectively, Using Aqueous Lithium Hydroxide. To a stirred solution of the ethyl cinnamate (1 mmol) in a 50:33:17 THF/MeOH/ H_2O mixture (16 mL) was added $LiOH \cdot H_2O$ (5 mmol). This mixture was stirred under argon, the reaction quenched with 2 N HCl to pH 1, and the mixture extracted (EtOAc). The extract was washed (brine) and dried. The residue obtained by concentration was chromatographed or washed (hexane and CH_2Cl_2) to afford the cinnamic acid.

4-Iodo-2-trifluoromethylphenyl Bromide (17). A reported procedure⁴⁵ was modified with respect to workup. To a cold solution prepared by adding 4-bromo-3-(trifluoromethyl)aniline (5.0 g, 20.8 mmol) to prewarmed concentrated sulfuric acid (5 mL) and H_2O (18.5 mL) was added with vigorous stirring and cooling (ice-salt bath) a solution of $NaNO_2$ (1.56 g, 21.9 mmol) in H_2O (10 mL) over a 30 min period. The mixture was stirred for 28 min before a solution of KI (4.74 g, 28 mmol) in H_2O (3.5 mL) and copper powder (approximately 3 mg) were added. The reaction mixture was allowed to warm to room temperature via removal of the ice bath, stirred for 1.3 h, and then heated at $101^\circ C$ for 1 h, cooled, and extracted with EtOAc (280 mL). Extracts were washed (water and brine) and dried. After solvent removal at reduced pressure, the residue was chromatographed (hexane) to give 4.8 g (66%) of **17** as a white solid: mp $72-73^\circ C$ (lit.⁴⁵ $78-80^\circ C$); 1H NMR δ 7.46 (d, $J = 8.4$ Hz, 1H, 3-ArH), 7.73 (dd, $J = 8.4, 2.1$ Hz, 1H, 4-ArH), 8.0 (d, $J = 2.1$ Hz, 1H, 6-ArH).

2-Benzyloxy-5-bromobenzonitrile (19) (method A). Compound **18** (1.31 g, 6.60 mmol) on reaction for 23 h, workup, and chromatography (10 to 20% EtOAc/hexane) gave 1.99 g (100%) of **19** as an off-white solid: mp $72-74^\circ C$; IR 2907, 2229, 1486, 1282 cm^{-1} ; 1H NMR δ 5.23 (s, 2H, $PhCH_2$), 6.92 (d, $J = 9.0$ Hz, 1H, 3-ArH), 7.33–7.50 (m, 5H, C_6H_5), 7.61 (dd, $J = 9.0, 2.4$ Hz, 1H, 4-ArH), 7.71 (d, $J = 2.4$ Hz, 1H, 6-ArH); HRMS calcd for $C_{14}H_{10}BrNO$ [$M + Na$]⁺ 309.9838, found 309.8840.

Methyl 2-Benzyloxy-5-bromobenzoate (21) (method A). Methyl 5-bromo-2-hydroxybenzoate (**20**) (1.50 g, 6.17 mmol) on reaction for 19 h, workup, and chromatography (5 to 9% EtOAc/hexane) gave 1.98 g (100%) of **21** as a light yellow liquid: IR 2909, 1731, 1486, 1242 cm^{-1} ; 1H NMR δ 3.94 (s, 3H, CH_3), 5.20 (s, 2H, $ArCH_2$), 6.93 (d, $J = 9.0$ Hz, 1H, 3-ArH), 7.31–7.52 (m, 5H, C_6H_5), 7.55 (dd, $J = 9.0, 2.7$ Hz, 1H, 4-ArH), 7.97 (d, $J = 2.7$ Hz, 1H, 6-ArH); HRMS calcd for $C_{15}H_{13}BrO_3$ [$M + Na$]⁺ 342.9940, found 342.9945.

4-Bromo-3-methoxybenzaldehyde (23). A method different from that reported in ref 46 was used. To a solution of benzonitrile **22** (1.04 g, 4.90 mmol) in anhydrous PhMe (14 mL) at $-78^\circ C$ was added 1 M DIBAL (7.35 mmol) in CH_2Cl_2 (7.40 mL). The reaction mixture was stirred at $-78^\circ C$ for 0.5 h, warmed to room temperature, stirred for an additional 4.25 h, the reaction quenched with MeOH (4 mL), and the mixture stirred for 0.5 h. After addition of 10% H_2SO_4 (45 mL), the resulting solution was stirred for 1.75 h and then extracted with EtOAc (100 mL, 50 mL). After solvent removal at reduced pressure, the residue was chromatographed (10 to 16% EtOAc/hexane) to give 876 mg (83%) of **23** as a white solid: mp $70-72^\circ C$ (lit.⁴⁶ $74-76^\circ C$); IR 2960, 1701, 1582, 1042 cm^{-1} ; 1H NMR δ 4.01 (s, 3H, CH_3), 7.36 (dd, $J = 1.8, 7.8$ Hz, 1H, 6-ArH), 7.43 (d, $J = 1.8$ Hz, 1H, 2-ArH), 7.77 (d, $J = 7.8$ Hz, 1H, 5-ArH), 9.98 (s, 1H, CHO).

Ethyl (E)-4-Bromo-3-(trifluoromethyl)cinnamate (25) (method B). 4-Iodo-2-trifluoromethylphenyl bromide (**17**) (1.0 g, 2.85 mmol) after coupling at $115^\circ C$ for 3 h, workup, and chromatography (10% EtOAc/hexane) produced 738 mg (80%) of **25** as a yellow solid: mp $92-94^\circ C$; IR 2917, 1704, 1362, 1174 cm^{-1} ; 1H NMR δ 1.38 (t, $J = 7.5$ Hz, 3H, OCH_2CH_3), 4.32 (q, $J = 7.5$ Hz, 2H, OCH_2CH_3), 6.53 (d,

$J = 15.9$ Hz, 1H, CH=CHCO), 7.55 (d, $J = 8.1$ Hz, 1H, 6-ArH), 7.67 (d, $J = 15.9$ Hz, 1H, CH=CHCO), 7.77 (d, $J = 8.1$ Hz, 1H, 5-ArH), 7.85 (s, 1H, 2-ArH); HRMS calcd for $C_{12}H_{10}BrF_3O_2$ $[M + H]^+$ 322.9889, found 322.9897.

Ethyl (E)-4-Benzyloxy-3-cyanocinnamate (26) (method B). 2-Benzyloxy-5-bromobenzonitrile (**19**) (1.97 g, 6.84 mmol) on coupling at 94 °C for 18 h, workup, and chromatography (5 to 33% EtOAc/hexane) produced 2.00 g (95%) of **26** as an off-white solid: mp 115–117 °C; IR 2924, 2230, 1707, 1501, 1268 cm^{-1} ; 1H NMR δ 1.38 (t, $J = 6.9$ Hz, 3H, OCH_2CH_3), 4.32 (q, $J = 6.9$ Hz, 2H, OCH_2CH_3), 5.29 (s, 2H, CH_2), 6.36 (d, $J = 15.9$ Hz, 1H, CH=CHCO), 7.05 (d, $J = 9.0$ Hz, 1H, 5-ArH), 7.33–7.51 (m, 5H, C_6H_5), 7.59 (d, $J = 15.9$ Hz, 1H, CH=CHCO), 7.67 (d, $J = 9.0$ Hz, 1H, 6-ArH), 7.77 (s, 1H, 2-ArH); HRMS calcd for $C_{19}H_{17}NO_3$ $[M + H]^+$ 308.1281, found 308.1285.

Ethyl (E)-3-Cyano-4-hydroxycinnamate (27) (method D). Ethyl (E)-4-benzyloxy-3-cyanocinnamate (**26**) (1.0 g, 3.25 mmol) after reaction for 2 h, workup, and chromatography (33 to 50% EtOAc/hexane) gave 0.7 g (99%) of **27** as an off-white solid: mp 198–200 °C; IR 3302, 2903, 2228, 1711, 1510 cm^{-1} ; 1H NMR δ 1.37 (t, $J = 7.5$ Hz, 3H, OCH_2CH_3), 4.30 (q, $J = 7.5$ Hz, 2H, OCH_2CH_3), 6.34 (s, 1H, OH), 6.37 (d, $J = 16.2$ Hz, 1H, CH=CHCO), 7.06 (d, $J = 8.4$ Hz, 1H, 5-ArH), 7.59 (d, $J = 16.2$ Hz, 1H, CH=CHCO), 7.67 (d, $J = 8.4$ Hz, 1H, 6-ArH), 7.69 (s, 1H, 2-ArH); HRMS calcd for $C_{12}H_{11}NO_3$ $[M + H]^+$ 218.0812, found 218.0811.

Ethyl (E)-3-Cyano-4-(trifluoromethylsulfonyloxy)cinnamate (28) (method E). Cinnamate **27** (685 mg, 3.15 mmol) after reaction for 24 h, workup, and chromatography (16.7% EtOAc/hexane) yielded 1.04 g (94%) of **28** as a white solid: mp 80–82 °C; IR 2903, 2226, 1705, 1236 cm^{-1} ; 1H NMR δ 1.37 (t, $J = 7.2$ Hz, 3H, OCH_2CH_3), 4.31 (q, $J = 7.2$ Hz, 2H, OCH_2CH_3), 6.51 (d, $J = 16.2$ Hz, 1H, CH=CHCO), 7.53 (d, $J = 8.4$ Hz, 1H, 5-ArH), 7.63 (d, $J = 16.2$ Hz, 1H, CH=CHCO), 7.85 (dd, $J = 8.4$, 2.1 Hz, 1H, 6-ArH), 7.90 (d, $J = 2.1$ Hz, 1H, 2-ArH); HRMS calcd for $C_{13}H_{10}F_3NO_5S$ $[M + H]^+$ 350.0305, found 350.0308.

Ethyl (E)-4-Benzyloxy-3-carbomethoxycinnamate (29) (method B). 4-Bromobenzoate **21** (1.10 g, 3.43 mmol) on coupling at 105 °C for 17 h, workup, and chromatography (5 to 22% EtOAc/hexane) produced 1.15 g (98%) of **29** as a pale yellow solid: mp 84–85 °C; IR 2902, 1729, 1689, 1501, 1269 cm^{-1} ; 1H NMR δ 1.36 (t, $J = 7.2$ Hz, 3H, OCH_2CH_3), 3.95 (s, 3H, CH_3), 4.29 (q, $J = 7.2$ Hz, 2H, OCH_2CH_3), 5.26 (s, 2H, $ArCH_2$), 6.39 (d, $J = 15.9$ Hz, 1H, CH=CHCO), 7.05 (d, $J = 8.4$ Hz, 1H, 5-ArH), 7.31–7.52 (m, 5H, C_6H_5), 7.60 (dd, $J = 8.4$, 2.4 Hz, 1H, 6-ArH), 7.67 (d, $J = 15.9$ Hz, 1H, CH=CHCO), 8.05 (d, $J = 2.4$ Hz, 1H, 2-ArH); HRMS calcd for $C_{20}H_{20}O_5$ $[M + H]^+$ 341.1383, found 341.1383.

Ethyl (E)-3-Carbomethoxy-4-hydroxycinnamate (30) (method D). Cinnamate **29** (623 mg, 1.83 mmol) after reaction for 2 h, workup, and chromatography (10 to 33% EtOAc/hexane) gave 456 mg (99%) of **30** as a pale yellow solid: mp 62–64 °C; IR 3247, 2941, 1707, 1677 cm^{-1} ; 1H NMR δ 1.36 (t, $J = 7.2$ Hz, 3H, OCH_2CH_3), 4.01 (s, 3H, CH_3), 4.29 (q, $J = 7.2$ Hz, 2H, OCH_2CH_3), 6.36 (d, $J = 16.2$ Hz, 1H, CH=CHCO), 7.03 (d, $J = 8.7$ Hz, 1H, 5-ArH), 7.64 (d, $J = 16.2$ Hz, 1H, CH=CHCO), 7.67 (d, $J = 8.7$ Hz, 1H, 6-ArH), 8.04 (s, 1H, 2-ArH), 11.0 (s, 1H, OH); HRMS calcd for $C_{13}H_{13}O_5$ $[M + H]^+$ 251.0914, found 251.0918.

Ethyl (E)-3-Carbomethoxy-4-(trifluoromethylsulfonyloxy)cinnamate (31) (method E). Cinnamate **30** (434 mg, 1.74 mmol) after reaction for 23 h, workup, and chromatography (10 to 16% EtOAc/hexane) yielded 641 mg (96%) of **31** as a white solid: mp 51–52 °C; IR 2913, 1731, 1431, 1213 cm^{-1} ; 1H NMR δ 1.39 (t, $J = 7.2$ Hz, 3H, OCH_2CH_3), 4.03 (s, 3H, CH_3), 4.33 (q, $J = 7.2$ Hz, 2H, OCH_2CH_3), 6.54 (d, $J = 16.2$ Hz, 1H, CH=CHCO), 7.36 (d, $J = 8.4$ Hz, 1H, 5-ArH), 7.69 (d, $J = 16.2$ Hz, 1H, CH=CHCO), 7.67 (dd, $J = 8.4$, 2.4 Hz, 1H, 6-ArH), 8.27 (d, $J = 2.4$ Hz, 1H, 2-ArH); HRMS calcd for $C_{14}H_{13}F_3O_7S$ $[M + H]^+$ 383.0407, found 383.0417.

Ethyl (E)-4-Bromo-3-methoxycinnamate (32) (method C). Benzaldehyde **23** (876 mg, 4.07 mmol) after reaction for 19 h, workup, and chromatography (10 to 16% EtOAc/hexane) produced 1.09 g (94%) of a cream solid (90% *E* isomer), which after crystallization (hexane) yielded 712 mg (61%) of the pure *E* isomer of **32** as a white solid:

mp 58–60 °C; IR 2988, 1709, 1484, 1177 cm^{-1} ; 1H NMR δ 1.36 (t, $J = 7.2$ Hz, 3H, OCH_2CH_3), 3.94 (s, 3H, OCH_3), 4.30 (q, $J = 7.2$ Hz, 2H, OCH_2CH_3), 6.54 (d, $J = 15.9$ Hz, 1H, CH=CHCO), 7.01 (d, $J = 8.1$ Hz, 1H, 6-ArH), 7.03 (s, 1H, 2-ArH), 7.56 (d, $J = 8.1$ Hz, 1H, 5-ArH), 7.64 (d, $J = 15.9$ Hz, 1H, CH=CHCO); HRMS calcd for $C_{12}H_{13}BrO_3$ $[M + H]^+$ 285.0121, found 285.0128.

Ethyl (E)-4-Bromo-3-nitrocinnamate (33) (method C). Benzaldehyde **24** (3.00 g, 13.03 mmol) after reaction for 18.5 h, workup, and chromatography (14 to 33% EtOAc/hexane) followed by crystallization (hexane) produced 3.36 g (86%) of **33** as a pale yellow solid: mp 132–134 °C; IR 2981, 1714, 1530, 1181 cm^{-1} ; 1H NMR δ 1.38 (t, $J = 7.2$ Hz, 3H, OCH_2CH_3), 4.31 (q, $J = 7.2$ Hz, 2H, OCH_2CH_3), 6.54 (d, $J = 16.2$ Hz, 1H, CH=CHCO), 7.58 (dd, $J = 2.1$, 8.4 Hz, 1H, 6-ArH), 7.65 (d, $J = 16.2$ Hz, 1H, CH=CHCO), 7.79 (d, $J = 8.4$ Hz, 1H, 5-ArH), 8.0 (d, $J = 2.1$ Hz, 1H, 2-ArH); HRMS calcd for $C_{11}H_{10}BrNO_4$ $[M + H]^+$ 299.9866, found 299.9865.

Ethyl (E)-4-[3'-(1-Adamantyl)-4'-benzyloxyphenyl]-3-(trifluoromethyl)cinnamate (35) (method F). Aryl halide **25** (194 mg, 0.6 mmol) on coupling for 18 h, workup, and chromatography (6 to 11% EtOAc/hexane) produced 319 mg (94%) of **35** as an off-white solid: mp 107–109 °C; IR 2903, 1713, 1124, 1176 cm^{-1} ; 1H NMR δ 1.39 (t, $J = 7.2$ Hz, 3H, OCH_2CH_3), 1.75 (bs, 6H, $AdCH_2$), 2.06 (bs, 3H, $AdCH$), 2.18 (bs, 6H, $AdCH_2$), 4.32 (q, $J = 7.2$ Hz, 2H, OCH_2CH_3), 5.19 (s, 2H, $ArCH_2$), 6.55 (d, $J = 16.2$ Hz, 1H, CH=CHCO), 7.01 (d, $J = 8.1$ Hz, 1H, 5'-ArH), 7.17 (dd, $J = 8.1$, 2.1 Hz, 1H, 6'-ArH), 7.25 (d, $J = 2.1$ Hz, 1H, 2'-ArH), 7.33–7.49 (m, 4H, 3H from C_6H_5 , 5-ArH), 7.54–7.57 (m, 2H, ArH), 7.71 (d, $J = 7.8$ Hz, 1H, 6-ArH), 7.77 (d, $J = 16.2$ Hz, 1H, CH=CHCO), 7.90 (s, 1H, 2-ArH); HRMS calcd for $C_{35}H_{35}F_3O_3$ $[M + H]^+$ 561.2611, found 561.2635.

Ethyl (E)-4-[3'-(1-Adamantyl)-4'-benzyloxyphenyl]-3-cyanocinnamate (36) (method G). Aryl triflate **28** (349 mg, 1.00 mmol) on coupling for 45 h, workup, and chromatography (9% EtOAc/hexane) produced 310 mg (60%) of **36** as an off-white solid: mp 65–67 °C; IR 2904, 2230, 1711, 1483, 1230 cm^{-1} ; 1H NMR δ 1.39 (t, $J = 7.2$ Hz, 3H, OCH_2CH_3), 1.77 (bs, 6H, $AdCH_2$), 2.08 (bs, 3H, $AdCH$), 2.23 (bs, 6H, $AdCH_2$), 4.33 (q, $J = 7.2$ Hz, 2H, OCH_2CH_3), 5.22 (s, 2H, CH_2), 6.53 (d, $J = 16.2$ Hz, 1H, CH=CHCO), 7.08 (d, $J = 8.4$ Hz, 1H, 5'-ArH), 7.35–7.58 (m, 5H, C_6H_5), 7.47 (dd, $J = 8.4$, 2.1 Hz, 1H, 6'-ArH), 7.52 (d, $J = 2.1$ Hz, 1H, 2'-ArH), 7.58 (d, $J = 8.4$ Hz, 1H, 5-ArH), 7.71 (d, $J = 16.2$ Hz, 1H, CH=CHCO), 7.78 (d, $J = 8.4$ Hz, 1H, 6-ArH), 7.90 (s, 1H, 2-ArH); HRMS calcd for $C_{35}H_{35}NO_3$ $[M + H]^+$ 518.2690, found 518.2686.

Ethyl (E)-4-[3'-(1-Adamantyl)-4'-benzyloxyphenyl]-3-carbomethoxycinnamate (37) (method G). Aryl triflate **31** (382 g, 1.0 mmol) on coupling for 22 h, workup, and chromatography (10 to 23% EtOAc/hexane) produced 546 mg (99%) of **37** as a white solid: mp 55–57 °C; IR 2905, 1712, 1479 cm^{-1} ; 1H NMR δ 1.38 (t, $J = 7.2$ Hz, 3H, OCH_2CH_3), 1.75 (bs, 6H, $AdCH_2$), 2.08 (bs, 3H, $AdCH$), 2.18 (bs, 6H, $AdCH_2$), 3.71 (s, 3H, CH_3), 4.31 (q, $J = 7.2$ Hz, 2H, OCH_2CH_3), 5.21 (s, 2H, $ArCH_2$), 6.53 (d, $J = 15.9$ Hz, 1H, CH=CHCO), 7.02 (d, $J = 8.1$ Hz, 1H, 5'-ArH), 7.20 (d, $J = 8.1$ Hz, 1H, 6'-ArH), 7.22 (s, 1H, 2'-ArH), 7.46 (d, $J = 7.8$ Hz, 1H, 5-ArH), 7.34–7.57 (m, 5H, C_6H_5), 7.67 (d, $J = 7.8$ Hz, 1H, 6-ArH), 7.74 (d, $J = 15.9$ Hz, 1H, CH=CHCO), 7.93 (s, 1H, 2-ArH); HRMS calcd for $C_{36}H_{38}O_5$ $[M + H]^+$ 551.2792, found 551.2789.

Ethyl (E)-4-[3'-(1-Adamantyl)-4'-benzyloxyphenyl]-3-methoxycinnamate (38) (method F). Aryl halide **32** (119 mg, 0.41 mmol) on coupling for 22.6 h, workup, and chromatography (11 to 12% EtOAc/hexane) produced 192 mg (88%) of **38** as a cream solid: mp 62–64 °C; IR 2903, 1706, 1487, 1163 cm^{-1} ; 1H NMR δ 1.39 (t, $J = 7.2$ Hz, 3H, OCH_2CH_3), 1.76 (bs, 6H, $AdCH_2$), 2.08 (bs, 3H, $AdCH$), 2.21 (bs, 6H, $AdCH_2$), 3.89 (s, 3H, OCH_3), 4.31 (q, $J = 7.2$ Hz, 2H, OCH_2CH_3), 5.19 (s, 2H, $ArCH_2$), 6.49 (d, $J = 15.9$ Hz, 1H, CH=CHCO), 7.01 (d, $J = 8.4$ Hz, 1H, 5'-ArH), 7.14 (s, 1H, 2'-ArH), 7.22 (dd, $J = 8.4$, 2.1 Hz, 1H, 6'-ArH), 7.31–7.58 (m, 8H, C_6H_5 , 2,5,6-ArH), 7.74 (d, $J = 15.9$ Hz, 1H, CH=CHCO); HRMS calcd for $C_{35}H_{38}O_4$ $[M + H]^+$ 523.2843, found 523.2842.

Ethyl (E)-4-[3'-(1-Adamantyl)-4'-benzyloxyphenyl]-3-nitrocinnamate (39) (method F). Aryl halide **33** (1.00 g, 3.33 mmol) on coupling for 16 h, workup, and chromatography (9 to 33% EtOAc/hexane)

produced 1.66 g (93%) of **39** as a yellow solid: mp 170–171 °C; IR 2902, 1719, 1532, 1179 cm⁻¹; ¹H NMR δ 1.39 (t, J = 7.2 Hz, 3H, OCH₂CH₃), 1.75 (bs, 6H, AdCH₂), 2.07 (bs, 3H, AdCH), 2.17 (bs, 6H, AdCH₂), 4.33 (q, J = 7.2 Hz, 2H, OCH₂CH₃), 5.19 (s, 2H, ArCH₂), 6.55 (d, J = 16.2 Hz, 1H, CH=CHCO), 7.03 (d, J = 8.4 Hz, 1H, 5'-ArH), 7.19 (dd, J = 8.4, 2.1 Hz, 1H, 6'-ArH), 7.24 (d, J = 2.1 Hz, 1H, 2'-ArH), 7.31–7.57 (m, 6H, C₆H₅, 5-ArH), 7.72 (d, J = 16.2 Hz, 1H, CH=CHCO), 7.74 (dd, J = 7.5, 1.5 Hz, 1H, 6-ArH), 7.94 (d, J = 1.5 Hz, 1H, 2-ArH); HRMS calcd for C₃₄H₃₅NO₅ [M + H]⁺ 538.2588, found 538.2584.

Ethyl (E)-4-[3'-(1-Adamantyl)-4'-hydroxyphenyl]-3-(trifluoromethyl)cinnamate (40) (method D). Cinnamate **35** (306 mg, 0.54 mmol) after reaction for 2 h, workup, and chromatography (9 to 14% EtOAc/hexane) gave 240 mg (93%) of **40** as a pale yellow solid: mp 186–187 °C; IR 3408, 2899, 1695, 1324, 1175 cm⁻¹; ¹H NMR δ 1.39 (t, J = 7.2 Hz, 3H, OCH₂CH₃), 1.81 (bs, 6H, AdCH₂), 2.11 (bs, 3H, AdCH), 2.16 (bs, 6H, AdCH₂), 4.32 (q, J = 7.2 Hz, 2H, OCH₂CH₃), 4.99 (s, 1H, OH), 6.55 (d, J = 16.2 Hz, 1H, CH=CHCO), 6.72 (d, J = 8.1 Hz, 1H, 5'-ArH), 7.06 (dd, J = 8.1, 1.8 Hz, 1H, 6'-ArH), 7.20 (d, J = 1.8 Hz, 1H, 2'-ArH), 7.40 (d, J = 8.1 Hz, 1H, 5-ArH), 7.71 (d, J = 8.1 Hz, 1H, 6-ArH), 7.76 (d, J = 16.2 Hz, 1H, CH=CHCO), 7.89 (s, 1H, 2-ArH); HRMS calcd for C₂₈H₂₉F₃O₃ [M + H]⁺ 471.2141, found 471.2151.

Ethyl (E)-4-[3'-(1-Adamantyl)-4'-hydroxyphenyl]-3-cyanocinnamate (41) (method D). Cinnamate **36** (147 mg, 0.28 mmol) after treatment for 2 h, workup, and chromatography (8 to 20% EtOAc/hexane) gave 102 mg (84%) of **41** as a cream solid: mp 220–222 °C; IR 3373, 2902, 2233, 1693, 1256 cm⁻¹; ¹H NMR (acetone-d₆) δ 1.33 (t, J = 7.2 Hz, 3H, OCH₂CH₃), 1.84 (bs, 6H, AdCH₂), 2.09 (bs, 3H, AdCH), 2.27 (bs, 6H, AdCH₂), 4.27 (q, J = 7.2 Hz, 2H, OCH₂CH₃), 6.75 (d, J = 16.2 Hz, 1H, CH=CHCO), 7.0 (d, J = 8.4 Hz, 1H, 5'-ArH), 7.38 (dd, J = 8.4, 2.1 Hz, 1H, 6'-ArH), 7.53 (d, J = 2.1 Hz, 1H, 2'-ArH), 7.69 (d, J = 8.1 Hz, 1H, 5-ArH), 7.76 (d, J = 16.2 Hz, 1H, CH=CHCO), 8.06 (dd, J = 8.1, 1.8 Hz, 1H, 6-ArH), 8.20 (d, J = 1.8 Hz, 1H, 2-ArH), 8.83 (s, 1H, OH); HRMS calcd for C₂₈H₂₉NO₃ [M + H]⁺ 428.2220, found 428.2214.

Ethyl (E)-4-[3'-(1-Adamantyl)-4'-hydroxyphenyl]-3-carbomethoxycinnamate (42) (method D). Cinnamate **37** (325 mg, 0.59 mmol) after reaction for 2 h, workup, and chromatography (10 to 33% EtOAc/hexane) gave 271 mg (100%) of **42** as a pale yellow solid: mp 71–73 °C; IR 3340, 2904, 1709, 1255 cm⁻¹; ¹H NMR δ 1.39 (t, J = 7.2 Hz, 3H, OCH₂CH₃), 1.81 (bs, 6H, AdCH₂), 2.12 (bs, 3H, AdCH), 2.16 (bs, 6H, AdCH₂), 3.72 (s, 3H, CH₃), 4.31 (q, J = 7.2 Hz, 2H, OCH₂CH₃), 4.97 (s, 1H, OH), 6.53 (d, J = 15.9 Hz, 1H, CH=CHCO), 6.72 (d, J = 8.1 Hz, 1H, 5'-ArH), 7.10 (dd, J = 8.1, 2.1 Hz, 1H, 6'-ArH), 7.18 (d, J = 2.1 Hz, 1H, 2'-ArH), 7.45 (d, J = 7.8 Hz, 1H, 5-ArH), 7.67 (dd, J = 7.8, 1.8 Hz, 1H, 6-ArH), 7.74 (d, J = 15.9 Hz, 1H, CH=CHCO), 7.93 (d, J = 1.8 Hz, 1H, 2-ArH); HRMS calcd for C₂₉H₃₃O₅ [M + H]⁺ 461.2328, found 461.2321.

Ethyl (E)-4-[3'-(1-Adamantyl)-4'-hydroxyphenyl]-3-methoxycinnamate (43) (method D). Cinnamate **38** (80 mg, 0.15 mmol) after reaction for 2 h, workup, and chromatography (16 to 33% EtOAc/hexane) gave 66 mg (100%) of **43** as a cream solid: mp 197–199 °C; IR 3332, 2902, 1686, 1493, 1183 cm⁻¹; ¹H NMR δ 1.39 (t, J = 7.5 Hz, 3H, OCH₂CH₃), 1.81 (bs, 6H, AdCH₂), 2.11 (bs, 3H, AdCH), 2.19 (bs, 6H, AdCH₂), 3.87 (s, 3H, OCH₃), 4.32 (q, J = 7.5 Hz, 2H, OCH₂CH₃), 5.37 (br s, 1H, OH), 6.49 (d, J = 15.9 Hz, 1H, CH=CHCO), 6.74 (d, J = 7.8 Hz, 1H, 5'-ArH), 7.12 (d, J = 1.5 Hz, 1H, 2'-ArH), 7.21 (dd, J = 1.5, 7.8 Hz, 1H, 6'-ArH), 7.31 (dd, J = 2.1, 8.1 Hz, 1H, 6-ArH), 7.35 (d, J = 8.1 Hz, 1H, 5-ArH), 7.42 (d, J = 2.1 Hz, 1H, 2-ArH), 7.74 (d, J = 15.9 Hz, 1H, CH=CHCO); HRMS calcd for C₂₈H₃₂O₄ [M + H]⁺ 433.2373, found 433.2370.

Ethyl (E)-4-[3'-(1-Adamantyl)-4'-hydroxyphenyl]-3-hydroxycinnamate (44) (method D). Cinnamate **38** (85 mg, 0.16 mmol) after reaction at -78 °C for 0.33 h and at room temperature for 2.5 h, workup, and chromatography (16 to 25% EtOAc/hexane) gave 43 mg (63%) of **44** as a yellow solid: mp 193–194 °C; IR 3295, 2838, 1693, 1463, 1216 cm⁻¹; ¹H NMR δ 1.39 (t, J = 7.2 Hz, 3H, OCH₂CH₃), 1.81 (bs, 6H, AdCH₂), 2.12 (bs, 3H, AdCH), 2.18 (bs, 6H, AdCH₂), 4.30 (q, J = 7.2 Hz, 2H, OCH₂CH₃), 5.49 (br s, 2H, OH), 6.47 (d, J = 15.9 Hz, 1H, CH=CHCO), 6.83 (d, J = 8.1 Hz, 1H, 5'-ArH), 7.12–7.22

(m, 3H, 2',6'-ArH, 5-ArH), 7.27 (dd, J = 2.1, 8.7 Hz, 1H, 6-ArH), 7.32 (d, J = 2.1 Hz, 1H, 2-ArH), 7.70 (d, J = 15.9 Hz, 1H, CH=CHCO); HRMS calcd for C₂₇H₃₀O₄ [M + H]⁺ 419.2217, found 419.2216.

Ethyl (E)-4-[3'-(1-Adamantyl)-4'-hydroxyphenyl]-3-nitrocinnamate (45) (method D). Cinnamate **39** (52 mg, 0.097 mmol) after treatment for 2 h, workup, and chromatography (16 to 20% EtOAc/hexane) gave 43 mg (100%) of **45** as a yellow solid: mp 236–238 °C; IR 3271, 2903, 1688, 1533, 1203 cm⁻¹; ¹H NMR δ 1.39 (t, J = 7.2 Hz, 3H, OCH₂CH₃), 1.81 (bs, 6H, AdCH₂), 2.12 (bs, 3H, AdCH), 2.15 (bs, 6H, AdCH₂), 4.32 (q, J = 7.2 Hz, 2H, OCH₂CH₃), 5.10 (br s, 1H, OH), 6.55 (d, J = 15.9 Hz, 1H, CH=CHCO), 6.73 (d, J = 8.1 Hz, 1H, 5'-ArH), 7.07 (dd, J = 1.8, 8.1 Hz, 1H, 6'-ArH), 7.2 (d, J = 2.1 Hz, 1H, 2'-ArH), 7.51 (d, J = 7.8 Hz, 1H, 5-ArH), 7.73 (d, J = 15.9 Hz, 1H, CH=CHCO), 7.73 (dd, J = 7.8, 1.5 Hz, 1H, 6-ArH), 7.93 (d, J = 1.5 Hz, 1H, 2-ArH); HRMS calcd for C₂₇H₂₉NO₅ [M + H]⁺ 448.2118, found 448.2117.

(E)-4-[3'-(1-Adamantyl)-4'-hydroxyphenyl]-3-(trifluoromethyl)cinnamic Acid (46) (method H). Cinnamate **40** (207 mg, 0.44 mmol) after hydrolysis for 35 min, workup, and chromatography (1:5:0 to 5:5:2 EtOAc/hexane/MeOH) afforded 164 mg (84%) of **46** as a pale yellow solid: mp 180–182 °C; IR 3239, 2900, 1686, 1317, 1140 cm⁻¹; ¹H NMR (CD₃OD) δ 1.84 (bs, 6H, AdCH₂), 2.07 (bs, 3H, AdCH), 2.20 (m, 6H, AdCH₂), 6.63 (d, J = 15.9 Hz, 1H, CH=CHCO), 6.79 (d, J = 8.4 Hz, 1H, 5'-ArH), 6.99 (dd, J = 8.1, 1.6 Hz, 1H, 6'-ArH), 7.12 (d, J = 1.6 Hz, 1H, 2'-ArH), 7.43 (d, J = 7.8 Hz, 1H, 5-ArH), 7.76 (d, J = 15.9 Hz, 1H, CH=CHCO), 7.88 (d, J = 7.8 Hz, 1H, 6-ArH), 7.96 (s, 1H, 2-ArH); HRMS calcd for C₂₆H₂₅F₃O₃ [M + H]⁺ 443.1828, found 443.1840.

(E)-4-[3'-(1-Adamantyl)-4'-hydroxyphenyl]-3-cyanocinnamic Acid (47) (method I). Cinnamate **41** (98 mg, 0.23 mmol) after hydrolysis for 5 h, workup, and washing (hexane and CH₂Cl₂) afforded 79 mg (86%) of **47** as a white solid: mp 294–296 °C; IR 3362, 2904, 2230, 1694, 1417, 1253 cm⁻¹; ¹H NMR (CD₃OD) δ 1.86 (bs, 6H, AdCH₂), 2.09 (bs, 3H, AdCH), 2.25 (bs, 6H, AdCH₂), 6.64 (d, J = 16.2 Hz, 1H, CH=CHCO), 6.88 (d, J = 8.1 Hz, 1H, 5'-ArH), 7.30 (d, J = 8.1 Hz, 1H, 6'-ArH), 7.46 (s, 1H, 2'-ArH), 7.62 (d, J = 8.4 Hz, 1H, 5-ArH), 7.72 (d, J = 16.2 Hz, 1H, CH=CHCO), 7.94 (d, J = 8.4 Hz, 1H, 6-ArH), 8.06 (s, 1H, 2-ArH); HRMS calcd for C₂₆H₂₅NO₃ [M + H]⁺ 400.1907, found 400.1903.

(E)-4-[3'-(1-Adamantyl)-4'-hydroxyphenyl]-3-(methoxycarbonyl)cinnamic Acid (48) (method H). Cinnamate **42** (231 mg, 0.48 mmol) after hydrolysis for 1.5 h, workup, and washing (hexane and CH₂Cl₂) afforded 190 mg (91%) of **48** as a white solid: mp 259–262 °C; IR 3347, 2906, 1712, 1695, 1253 cm⁻¹; ¹H NMR (CD₃OD) δ 1.84 (bs, 6H, AdCH₂), 2.08 (bs, 3H, AdCH), 2.19 (bs, 6H, AdCH₂), 3.69 (s, 3H, CH₃), 6.55 (d, J = 15.9 Hz, 1H, CH=CHCO), 6.79 (d, J = 8.1 Hz, 1H, 5'-ArH), 7.04 (dd, J = 8.1, 2.4 Hz, 1H, 6'-ArH), 7.08 (d, J = 2.4 Hz, 1H, 2'-ArH), 7.48 (d, J = 8.1 Hz, 1H, 5-ArH), 7.74 (d, J = 15.9 Hz, 1H, CH=CHCO), 7.80 (dd, J = 8.1, 1.4 Hz, 1H, 6-ArH), 7.86 (d, J = 1.4 Hz, 1H, 2-ArH); HRMS calcd for C₂₇H₂₈O₅ [M + H]⁺ 433.2009, found 433.2011.

(E)-4-[3'-(1-Adamantyl)-4'-hydroxyphenyl]-3-carboxycinnamic Acid (49). To a solution of **48** (61 mg, 0.14 mmol) in a THF/MeOH/H₂O mixture (3:2:1, 1.8 mL) was added lithium hydroxide monohydrate (30 mg, 0.71 mmol). This mixture was stirred under argon for 21 h at which time TLC indicated some starting material **48**. Therefore, the mixture was treated with MeOH (2 mL) and 5 N aqueous NaOH (0.4 mL) at 82 °C for 24 h, the reaction quenched with 1 N HCl (6 mL), and the mixture extracted with EtOAc (40 and 20 mL). The extract was washed (brine), dried, and concentrated at reduced pressure. The residue was washed with hexane, CH₂Cl₂ (three times), and pentane and dried to give 42 mg (71%) of **49** as a cream solid: mp 274–277 °C; IR 3281, 2895, 1712, 1691, 1250 cm⁻¹; ¹H NMR (CD₃OD) δ 1.83 (bs, 6H, AdCH₂), 2.07 (bs, 3H, AdCH), 2.20 (bs, 6H, AdCH₂), 6.56 (d, J = 15.9 Hz, 1H, CH=CHCO), 6.78 (d, J = 8.1 Hz, 1H, 5'-ArH), 7.10 (d, J = 8.1 Hz, 1H, 6'-ArH), 7.20 (s, 1H, 2'-ArH), 7.45 (d, J = 7.5 Hz, 1H, 5-ArH), 7.73 (d, J = 15.9 Hz, 1H, CH=CHCO), 7.75 (d, J = 7.5 Hz, 1H, 6-ArH), 7.86 (s, 1H, 2-ArH); HRMS calcd for C₂₆H₂₆O₅ [M + H]⁺ 419.1853, found 419.1855.

(*E*)-4-[3'-(1-Adamantyl)-4'-hydroxyphenyl]-3-methoxycinnamic Acid (**50**) (method I). Cinnamate **43** (66 mg, 0.15 mmol) on hydrolysis for 6.3 h, workup, and washing (hexane and CH₂Cl₂) afforded 43 mg (70%) of **50** as a cream solid: mp 218–220 °C; IR 3281, 2905, 1686, 1421, 1252 cm⁻¹; ¹H NMR (CD₃OD) δ 1.79 (bs, 6H, AdCH₂), 2.03 (bs, 3H, AdCH), 2.16 (bs, 6H, AdCH₂), 3.82 (s, 3H, CH₃O), 6.47 (d, *J* = 15.9 Hz, 1H, CH=CHCO), 6.70 (d, *J* = 8.5 Hz, 1H, 5'-ArH), 7.13 (dd, *J* = 8.5, 1.8 Hz, 1H, 6'-ArH), 7.20 (dd, *J* = 8.7, 2.4 Hz, 1H, 6-ArH), 7.22 (d, *J* = 1.8 Hz, 1H, 2'-ArH), 7.25 (d, *J* = 8.7 Hz, 1H, 5-ArH), 7.27 (d, *J* = 2.4 Hz, 1H, 2-ArH), 7.66 (d, *J* = 15.9 Hz, 1H, CH=CHCO); HRMS calcd for C₂₆H₂₈O₄ [M + H]⁺ 405.2060, found 405.2056.

(*E*)-4-[3'-(1-Adamantyl)-4'-hydroxyphenyl]-3-hydroxycinnamic Acid (**51**) (method H). Cinnamate **44** (35 mg, 0.08 mmol) after hydrolysis for 1.5 h, workup, and washing (hexane and CH₂Cl₂) afforded 28 mg (85%) of **51** as a light yellow solid: mp >260 °C dec; IR 3276, 2907, 1689, 1429, 1177 cm⁻¹; ¹H NMR (CDCl₃/CD₃OD) δ 1.54 (bs, 6H, AdCH₂), 1.82 (bs, 3H, AdCH), 1.94 (bs, 6H, AdCH₂), 6.14 (d, *J* = 15.9 Hz, 1H, CH=CHCO), 6.83 (d, *J* = 7.5 Hz, 1H, 5'-ArH), 6.84 (dd, *J* = 7.5, 1.8 Hz, 1H, 6'-ArH), 6.86 (d, *J* = 1.8 Hz, 1H, 2'-ArH), 7.03 (dd, *J* = 8.5, 1.8 Hz, 1H, 6-ArH), 7.04 (d, *J* = 8.5 Hz, 1H, 5-ArH), 7.13 (d, *J* = 1.8 Hz, 1H, 2-ArH), 7.38 (d, *J* = 15.9 Hz, 1H, CH=CHCO); HRMS calcd for C₂₅H₂₆O₄ [M + H]⁺ 391.1904, found 391.1906.

(*E*)-4-[3'-(1-Adamantyl)-4'-hydroxyphenyl]-3-nitrocinnamic Acid (**52**) (method I). Cinnamate **45** (36 mg, 0.08 mmol) after hydrolysis for 3.5 h, workup, and washing (hexane and CH₂Cl₂) afforded 32 mg (95%) of **52** as a yellow solid: mp 285–287 °C; IR 3278, 2904, 1696, 1529, 1254 cm⁻¹; ¹H NMR (CD₃OD) δ 1.84 (bs, 6H, AdCH₂), 2.08 (bs, 3H, AdCH), 2.18 (m, 6H, AdCH₂), 6.65 (d, *J* = 16.2 Hz, 1H, CH=CHCO), 6.80 (d, *J* = 8.1 Hz, 1H, 5'-ArH), 7.04 (dd, *J* = 8.1, 2.1 Hz, 1H, 6'-ArH), 7.10 (d, *J* = 2.1 Hz, 1H, 2'-ArH), 7.54 (d, *J* = 7.8 Hz, 1H, 5-ArH), 7.74 (d, *J* = 16.2 Hz, 1H, CH=CHCO), 7.88 (dd, *J* = 7.8, 1.8 Hz, 1H, 6-ArH), 8.01 (d, *J* = 1.8 Hz, 1H, 2-ArH); HRMS calcd for C₂₅H₂₅NO₅ [M + H]⁺ 420.1805, found 420.1800.

Ethyl (*E*)-4-[3'-(1-Adamantyl)-4'-benzyloxyphenyl]-3-aminocinnamate (**53**). A suspension of **39** (538 mg, 1.00 mmol) and stannous chloride dihydrate (1.13 g, 5.00 mmol) in EtOH (4.5 mL) was heated at 80 °C (oil bath) for 2 h. Next, most of the solvent was removed at reduced pressure; the mixture was cooled to room temperature, and its pH was adjusted to 7–8 by addition of 2 N NaOH (4 mL) and 5% NaHCO₃ (10 mL). The resulting mixture was stirred for 10 min and then extracted with EtOAc (80 mL and 2 × 50 mL). The residue obtained after workup was purified by chromatography on silica gel (14 to 50% EtOAc/hexane) to give 506 mg (99%) of **53** as a pale yellow solid: mp 150–151 °C; IR 3370, 2905, 1703, 1177 cm⁻¹; ¹H NMR (CDCl₃) δ 1.38 (t, *J* = 7.2 Hz, 3H, OCH₂CH₃), 1.76 (bs, 6H, AdCH₂), 2.08 (bs, 3H, AdCH), 2.20 (bs, 6H, AdCH₂), 3.89 (bs, 2H, NH₂), 4.30 (q, *J* = 7.2 Hz, 2H, OCH₂CH₃), 5.20 (s, 2H, CH₂), 6.43 (d, *J* = 15.9 Hz, 1H, CH=CHCO), 6.94 (s, 1H, 2-ArH), 7.02 (d, *J* = 8.1 Hz, 1H, 6-ArH), 7.05 (d, *J* = 8.1 Hz, 1H, 5-ArH), 7.18 (d, *J* = 7.8 Hz, 1H, 5'-ArH), 7.27 (dd, *J* = 8.1, 2.1 Hz, 1H, 6'-ArH), 7.36 (d, *J* = 2.1 Hz, 1H, 2'-ArH), 7.32–7.58 (m, 5H, ArH), 7.65 (d, *J* = 15.9 Hz, 1H, CH=CHCO); HRMS calcd for C₃₄H₃₇NO₃ [M + H]⁺ 508.2846, found 508.2847.

Ethyl (*E*)-4-[3'-(1-Adamantyl)-4'-benzyloxyphenyl]-3-bromocinnamate (**54**). To a solution of *n*-hexyl nitrite (32 mg, 0.24 mmol) in CHBr₃ (0.6 mL) at 95 °C was added **53** (1.408 g, 4.64 mL) in CHBr₃ (4.5 mL) over a period of 5 min. The mixture was stirred at 100 °C for 5 h and cooled to room temperature. After most of the CHBr₃ had been removed under high vacuum, the residue was purified on silica gel (3 to 5% EtOAc/hexane) to give 67 mg (58%) of **54** as a white solid: mp 159–161 °C; IR 2903, 1712, 1230 cm⁻¹; ¹H NMR (CDCl₃) δ 1.39 (t, *J* = 7.2 Hz, 3H, OCH₂CH₃), 1.76 (bs, 6H, AdCH₂), 2.08 (bs, 3H, AdCH), 2.21 (bs, 6H, AdCH₂), 4.31 (q, *J* = 7.2 Hz, 2H, OCH₂CH₃), 5.20 (s, 2H, ArCH₂), 6.48 (d, *J* = 15.9 Hz, 1H, CH=CHCO), 7.03 (d, *J* = 8.4 Hz, 1H, 5'-ArH), 7.28 (dd, *J* = 8.4, 2.4 Hz, 1H, 6'-ArH), 7.38 (d, *J* = 2.4 Hz, 1H, 2'-ArH), 7.39 (d, *J* = 7.8 Hz, 1H, 5-ArH), 7.51 (dd, *J* = 7.8, 1.5 Hz, 1H, 6-ArH), 7.32–7.57 (m, 6H, ArH, 5-ArH), 7.67 (d, *J* = 15.9 Hz, 1H, CH=CHCO), 7.86 (d, *J* = 1.5

Hz, 1H, 2-ArH); HRMS calcd for C₃₄H₃₅BrO₃ [M + H]⁺ 571.1842, found 571.1838.

Ethyl (*E*)-4-[3'-(1-Adamantyl)-4'-benzyloxyphenyl]-3,6-dibromocinnamate (**55**). To a solution of **53** (228 mg, 0.45 mmol) in anhydrous MeCN (2 mL) at 0 °C were added, under argon, *tert*-butyl nitrite (107 μL, 0.9 mmol) and CuBr₂ (201 mg, 0.9 mmol). The mixture was stirred at 0 °C for 45 min, warmed to room temperature, stirred for 4 h, the reaction quenched with 1 N HCl (20 mL), and the mixture extracted with EtOAc (60 and 40 mL). The residue obtained on workup was chromatographed (3 to 5% EtOAc/hexane) to give 135 mg (46%) of **55** as a pale yellow solid: mp 74–77 °C; IR 2907, 1718, 1457, 1183 cm⁻¹; ¹H NMR δ 1.38 (t, *J* = 7.2 Hz, 3H, OCH₂CH₃), 1.76 (bs, 6H, AdCH₂), 2.08 (bs, 3H, AdCH), 2.20 (bs, 6H, AdCH₂), 4.32 (q, *J* = 7.2 Hz, 2H, OCH₂CH₃), 5.20 (s, 2H, CH₂), 6.45 (d, *J* = 15.9 Hz, 1H, CH=CHCO), 7.02 (d, *J* = 8.4 Hz, 1H, 5'-ArH), 7.24 (dd, *J* = 8.4, 2.1 Hz, 1H, 6'-ArH), 7.34 (d, *J* = 2.1 Hz, 1H, 2'-ArH), 7.32–7.58 (m, 5H, ArH), 7.62 (s, 1H, 5-ArH), 7.92 (s, 1H, 2-ArH), 8.01 (d, *J* = 15.9 Hz, 1H, CH=CHCO); HRMS calcd for C₃₄H₃₄Br₂O₃ [M + H]⁺ 649.0947, found 649.0943.

Ethyl (*E*)-4-[3'-(1-Adamantyl)-4'-hydroxyphenyl]-3-aminocinnamate (**56**) (method D). A solution of **53** (45 mg, 0.089 mmol) after reaction for 2.5 h, workup, and chromatography (16 to 20% EtOAc/hexane) gave 30 mg (81%) of **56** as a light yellow solid: mp 214–216 °C; IR 3356, 2905, 1692, 1178 cm⁻¹; ¹H NMR δ 1.38 (t, *J* = 7.2 Hz, 3H, OCH₂CH₃), 1.81 (bs, 6H, AdCH₂), 2.12 (bs, 3H, AdCH), 2.17 (bs, 6H, AdCH₂), 3.80 (bs, 2H, NH₂), 4.29 (q, *J* = 7.2 Hz, 2H, OCH₂CH₃), 5.03 (bs, 1H, OH), 6.43 (d, *J* = 16.2 Hz, 1H, CH=CHCO), 6.76 (d, *J* = 8.1 Hz, 1H, 5'-ArH), 6.94 (d, *J* = 1.5 Hz, 1H, 2'-ArH), 7.01 (dd, *J* = 8.1, 1.5 Hz, 1H, 6'-ArH), 7.16 (d, *J* = 7.5 Hz, 1H, 5-ArH), 7.19 (dd, *J* = 2.1, 7.5 Hz, 1H, 6-ArH), 7.32 (d, *J* = 2.1 Hz, 1H, 2-ArH), 7.65 (d, *J* = 16.2 Hz, 1H, CH=CHCO); HRMS calcd for C₂₇H₃₁NO₃ [M + H]⁺ 418.2377, found 418.2372.

(*E*)-4-[3'-(1-Adamantyl)-4'-hydroxyphenyl]-3-aminocinnamic Acid (**57**) (method I). Cinnamate **56** (27 mg, 0.065 mmol) after hydrolysis for 4 h, workup, and washing (hexane, CH₂Cl₂, and pentane) afforded 25 mg (100%) of **57** as a yellow solid: mp 240–242 °C; IR 3360, 2902, 1687, 1253 cm⁻¹; ¹H NMR (CD₃OD) δ 1.84 (bs, 6H, AdCH₂), 2.08 (bs, 3H, AdCH), 2.21 (bs, 6H, AdCH₂), 6.43 (d, *J* = 15.9 Hz, 1H, CH=CHCO), 6.82 (d, *J* = 8.4 Hz, 1H, 5'-ArH), 7.01 (dd, *J* = 8.4, 1.5 Hz, 1H, 6'-ArH), 7.06 (d, *J* = 1.5 Hz, 1H, 2'-ArH), 7.08 (d, *J* = 8.1 Hz, 1H, 5-ArH), 7.10 (dd, *J* = 8.1, 2.1 Hz, 1H, 6-ArH), 7.21 (d, *J* = 2.1 Hz, 1H, 2-ArH), 7.62 (d, *J* = 15.9 Hz, 1H, CH=CHCO); HRMS calcd for C₂₅H₂₇NO₃ [M + H]⁺ 390.2064, found 390.2065.

Ethyl (*E*)-4-[3'-(1-Adamantyl)-4'-hydroxyphenyl]-3-azidocinnamate (**58**). To a suspension of **56** (100 mg, 0.197 mmol) in 1,4-dioxane (1.2 mL) and 2 M H₂SO₄ (2.5 mL) at -10 to -5 °C under argon was added a solution of NaNO₂ (30 mg, 0.43 mmol) in H₂O (140 μL). The mixture was stirred at -10 to -5 °C for 20 min before a solution of NaN₃ (43 mg, 0.65 mmol) in H₂O (220 μL) was added, and stirring was continued for 30 min. The mixture was warmed to room temperature and diluted with EtOAc (70 mL). The organic layer was washed (saturated NaHCO₃ and brine), dried, and concentrated at reduced pressure. The residue was chromatographed (10 to 14% EtOAc/hexane) to give 76 mg (87%, two steps from **53**) of **58** as a light yellow solid: mp 88–91 °C; IR 3416, 2901, 2111, 1691, 1180 cm⁻¹; ¹H NMR (CDCl₃) δ 1.35 (t, *J* = 7.2 Hz, 3H, OCH₂CH₃), 1.78 (bs, 6H, AdCH₂), 2.09 (bs, 3H, AdCH), 2.15 (bs, 6H, AdCH₂), 3.80 (bs, 2H, NH₂), 4.28 (q, *J* = 7.2 Hz, 2H, OCH₂CH₃), 5.14 (bs, 1H, OH), 6.46 (d, *J* = 16.2 Hz, 1H, CH=CHCO), 6.76 (d, *J* = 8.4 Hz, 1H, 5'-ArH), 7.18 (dd, *J* = 8.4, 2.1 Hz, 1H, 6'-ArH), 7.28 (d, *J* = 2.1 Hz, 1H, 2'-ArH), 7.33 (bs, 3H, 2,5,6-ArH), 7.66 (d, *J* = 16.2 Hz, 1H, CH=CHCO); HRMS calcd for C₂₇H₂₉N₃O₃ [M + H]⁺ 444.2282, found 444.2281.

(*E*)-4-[3'-(1-Adamantyl)-4'-hydroxyphenyl]-3-azidocinnamic Acid (**59**). To a suspension of **58** (53 mg, 0.12 mmol) in Et₂O (0.1 mL) and EtOH (0.2 mL) was added 25% aqueous NaOH (50 μL, 0.42 mmol). The mixture was stirred for 6 h, acidified with 1 N HCl (10 mL), and extracted with EtOAc (50 and 30 mL). The extract was washed (brine), dried, and concentrated at reduced pressure. The

residue was chromatographed (0:50:50 to 14:43:43 MeOH/EtOAc/hexane) to give 33 mg (66%) of **59** as a tan solid: mp >260 °C; IR 3374, 2904, 2113, 1685, 1251 cm⁻¹; ¹H NMR (DMSO-*d*₆) δ 1.76 (bs, 6H, AdCH₂), 2.07 (bs, 3H, AdCH), 2.13 (bs, 6H, AdCH₂), 6.65 (d, *J* = 16.2 Hz, 1H, CH=CHCO), 6.85 (d, *J* = 8.7 Hz, 1H, 5'-ArH), 7.19 (m, 2H, 2',6'-ArH), 7.38 (d, *J* = 7.8 Hz, 1H, 5-ArH), 7.57 (d, *J* = 7.8 Hz, 1H, 6-ArH), 7.66 (d, *J* = 16.2 Hz, 1H, CH=CHCO), 7.67 (s, 1H, 2-ArH), 9.58 (s, 1H, OH), 12.43 (bs, 1H, COOH); HRMS calcd for C₂₅H₂₅N₃O₃ [M + H]⁺ 416.1974, found 416.1988.

Ethyl (E)-4-[3'-(1-Adamantyl)-4'-hydroxyphenyl]-3-bromocinnamate (60) (method D). Cinnamate **54** (67 mg, 0.12 mmol) after reaction for 2 h, workup, and chromatography (9 to 11% EtOAc/hexane) gave 51 mg (90%) of **60** as a cream solid: mp 213–215 °C; IR 3351, 2903, 1691, 1197 cm⁻¹; ¹H NMR δ 1.39 (t, *J* = 7.2 Hz, 3H, OCH₂CH₃), 1.82 (bs, 6H, AdCH₂), 2.13 (bs, 3H, AdCH), 2.19 (bs, 6H, AdCH₂), 4.31 (q, *J* = 7.2 Hz, 2H, OCH₂CH₃), 5.01 (s, 1H, OH), 6.48 (d, *J* = 15.9 Hz, 1H, CH=CHCO), 6.74 (d, *J* = 8.1 Hz, 1H, 5'-ArH), 7.18 (dd, *J* = 8.1, 2.1 Hz, 1H, 6'-ArH), 7.33 (d, *J* = 2.1 Hz, 1H, 2'-ArH), 7.38 (d, *J* = 8.1 Hz, 1H, 5-ArH), 7.51 (dd, *J* = 8.1, 1.8 Hz, 1H, 6-ArH), 7.67 (d, *J* = 15.9 Hz, 1H, CH=CHCO), 7.86 (d, *J* = 1.8 Hz, 1H, 2-ArH); HRMS calcd for C₂₇H₂₉BrO₃ [M + H]⁺ 481.1373, found 481.1374.

(E)-4-[3'-(1-Adamantyl)-4'-hydroxyphenyl]-3-bromocinnamic Acid (61) (method I). Cinnamate **60** (30 mg, 0.06 mmol) after hydrolysis for 5 h, workup, and washing (hexane and CH₂Cl₂) afforded 25 mg (89%) of **61** as a cream solid: mp 244–247 °C; IR 3313, 2915, 1702, 1166 cm⁻¹; ¹H NMR (CD₃OD) δ 1.84 (bs, 6H, AdCH₂), 2.08 (bs, 3H, AdCH), 2.21 (bs, 6H, AdCH₂), 6.54 (d, *J* = 16.2 Hz, 1H, CH=CHCO), 6.79 (d, *J* = 8.1 Hz, 1H, 5'-ArH), 7.08 (dd, *J* = 8.1, 2.1 Hz, 1H, 6'-ArH), 7.22 (d, *J* = 2.1 Hz, 1H, 2'-ArH), 7.38 (d, *J* = 8.1 Hz, 1H, 5-ArH), 7.62 (dd, *J* = 8.1, 1.5 Hz, 1H, 6-ArH), 7.67 (d, *J* = 16.2 Hz, 1H, CH=CHCO), 7.92 (d, *J* = 1.5 Hz, 1H, 2-ArH); HRMS calcd for C₂₅H₂₃BrO₃ [M + H]⁺ 453.1060, found 453.1062.

Ethyl (E)-4-[3'-(1-Adamantyl)-4'-hydroxyphenyl]-3,6-dibromocinnamate (62) (method D). Cinnamate **55** (128 mg, 0.20 mmol) after reaction for 2 h, workup, and chromatography (4 to 12% EtOAc/hexane) gave 97 mg (88%) of **62** as a pale yellow solid: mp 211–213 °C; IR 3382, 2905, 1694, 1194 cm⁻¹; ¹H NMR δ 1.39 (t, *J* = 7.2 Hz, 3H, OCH₂CH₃), 1.82 (bs, 6H, AdCH₂), 2.13 (bs, 3H, AdCH), 2.18 (bs, 6H, AdCH₂), 4.33 (q, *J* = 7.2 Hz, 2H, OCH₂CH₃), 5.03 (s, 1H, OH), 6.45 (d, *J* = 15.9 Hz, 1H, CH=CHCO), 6.74 (d, *J* = 8.4 Hz, 1H, 5'-ArH), 7.15 (dd, *J* = 8.4, 2.1 Hz, 1H, 6'-ArH), 7.30 (d, *J* = 2.1 Hz, 1H, 2'-ArH), 7.61 (s, 1H, 5-ArH), 7.91 (s, 1H, 2-ArH), 8.01 (d, *J* = 15.9 Hz, 1H, CH=CHCO); HRMS calcd for C₂₇H₂₈Br₂O₃ [M + H]⁺ 559.0478, found 559.0468.

(E)-4-[3'-(1-Adamantyl)-4'-hydroxyphenyl]-3,6-dibromocinnamic Acid (63) (method I). Cinnamate **62** (58 mg, 0.104 mmol) upon hydrolysis for 3.5 h, workup, and washing (hexane, CH₂Cl₂, and CHCl₃) afforded 53 mg (96%) of **63** as a yellow solid: mp 262–264 °C; IR 3299, 2904, 1701, 1249 cm⁻¹; ¹H NMR (CD₃OD) δ 1.84 (bs, 6H, AdCH₂), 2.08 (bs, 3H, AdCH), 2.21 (bs, 6H, AdCH₂), 6.55 (d, *J* = 15.9 Hz, 1H, CH=CHCO), 6.80 (d, *J* = 8.4 Hz, 1H, 5'-ArH), 7.08 (dd, *J* = 8.4, 2.1 Hz, 1H, 6'-ArH), 7.21 (d, *J* = 2.1 Hz, 1H, 2'-ArH), 7.61 (s, 1H, 5-ArH), 7.97 (d, *J* = 15.9 Hz, 1H, CH=CHCO), 8.07 (s, 1H, 2-ArH); HRMS calcd for C₂₅H₂₄Br₂O₃ [M + H]⁺ 531.0165, found 531.0171.

Ethyl (E)-3-[6-(1-Adamantyl)-7-benzyloxy-9H-carbazol-2-yl]propenoate (64) and Ethyl (E)-3-[8-(1-Adamantyl)-7-benzyloxy-9H-carbazol-2-yl]propenoate (67). A reported method was used to synthesize carbazoles **64** and **67**.^{18,19} To a solution of **39** (0.80 g, 1.49 mmol) in 1,2-dichlorobenzene was added PPh₃ (0.97 g, 3.72 mmol). The mixture was heated at 180 °C while being stirred under argon for 19 h. After cooling, the mixture was chromatographed (9 to 25% EtOAc/hexane) to give fractions containing **64** or **67**, as the major isomer, each of which was separately crystallized (EtOH, 6 mL) to afford 390 mg (52%) of **64** as a yellow solid: mp 203–205 °C, and 330 mg (44%) of **67** as a yellow solid: mp 144–145 °C. **64**: IR 3334, 2905, 1704, 1291 cm⁻¹; ¹H NMR δ 1.38 (t, *J* = 7.2 Hz, 3H, OCH₂CH₃), 1.79 (bs, 6H, AdCH₂), 2.12 (bs, 3H, AdCH), 2.28 (bs,

6H, AdCH₂), 4.31 (q, *J* = 7.2 Hz, 2H, OCH₂CH₃), 5.25 (s, 2H, ArCH₂), 6.51 (d, *J* = 16.2 Hz, 1H, CH=CHCO), 6.99 (s, 1H, 8H-carbazole), 7.36–7.60 (m, 7H, C₅H₅, 1H, 3H-carbazole), 7.86 (d, *J* = 16.2 Hz, 1H, CH=CHCO), 7.94 (s, 1H, 5H-carbazole), 7.97 (bs, 1H, 9H-carbazole), 7.99 (d, *J* = 7.8 Hz, 1H, 4H-carbazole); HRMS calcd for C₃₄H₃₅NO₃ [M + H]⁺ 506.2690, found 506.2683. **67**: IR 3407, 2911, 1702, 1272 cm⁻¹; ¹H NMR δ 1.39 (t, *J* = 7.2 Hz, 3H, OCH₂CH₃), 1.80 (bs, 6H, AdCH₂), 2.12 (bs, 3H, AdCH), 2.61 (bs, 6H, AdCH₂), 4.32 (q, *J* = 7.2 Hz, 2H, OCH₂CH₃), 5.24 (s, 2H, ArCH₂), 6.53 (d, *J* = 15.9 Hz, 1H, CH=CHCO), 7.03 (d, *J* = 8.4 Hz, 1H, 6H-carbazole), 7.35–7.59 (m, 7H, C₅H₅, 1H, 3H-carbazole), 7.85 (d, *J* = 16.2 Hz, 1H, CH=CHCO), 7.88 (d, *J* = 8.4 Hz, 1H, 5H-carbazole), 7.95 (d, *J* = 8.1 Hz, 1H, 4H-carbazole), 8.91 (bs, 1H, 9H-carbazole); HRMS calcd for C₃₄H₃₅NO₃ [M + H]⁺ 506.2690, found 506.2688.

Ethyl (E)-3-[6-(1-Adamantyl)-7-hydroxy-9H-carbazol-2-yl]propenoate (65) (method D). Ester **64** (100 mg, 0.20 mmol) after reaction for 2.3 h, workup, and chromatography (16 to 28% EtOAc/hexane) gave 60 mg (73%) of **65** as a yellow solid: mp 244–246 °C; IR 3311, 2915, 1670, 1249 cm⁻¹; ¹H NMR δ 1.39 (t, *J* = 7.2 Hz, 3H, OCH₂CH₃), 1.86 (bs, 6H, AdCH₂), 2.17 (bs, 3H, AdCH), 2.27 (bs, 6H, AdCH₂), 4.32 (q, *J* = 7.2 Hz, 2H, OCH₂CH₃), 5.25 (s, 1H, OH), 6.50 (d, *J* = 15.9 Hz, 1H, CH=CHCO), 6.73 (s, 1H, 8H-carbazole), 7.43 (dd, *J* = 8.1, 1.2 Hz, 1H, 3H-carbazole), 7.46 (s, 1H, 1H-carbazole), 7.84 (d, *J* = 15.9 Hz, 1H, CH=CHCO), 7.86 (bs, 1H, 9H-carbazole), 7.91 (s, 1H, 5H-carbazole), 7.97 (d, *J* = 8.1 Hz, 1H, 4H-carbazole); HRMS calcd for C₂₇H₂₉NO₃ [M + H]⁺ 416.2226, found 416.2224.

(E)-3-[8-(1-Adamantyl)-7-hydroxy-9H-carbazol-2-yl]propenoic Acid (66) (method I). Ester **65** (42 mg, 0.10 mmol) upon hydrolysis for 23 h, workup, and chromatography (0:67:33 to 6.5:93.5:0 MeOH/EtOAc/hexane) afforded 15 mg (38%) of **66** as a yellow solid: mp 256–258 °C; IR 3334, 2905, 1685, 1280 cm⁻¹; ¹H NMR (acetone-*d*₆) δ 1.87 (bs, 6H, AdCH₂), 2.13 (bs, 3H, AdCH), 2.33 (bs, 6H, AdCH₂), 6.55 (d, *J* = 15.9 Hz, 1H, CH=CHCO), 7.00 (s, 1H, 8H-carbazole), 7.48 (dd, *J* = 8.1, 1.5 Hz, 1H, 3H-carbazole), 7.71 (d, *J* = 1.5 Hz, 1H, 1H-carbazole), 7.84 (d, *J* = 15.9 Hz, 1H, CH=CHCO), 7.93 (s, 1H, 5H-carbazole), 8.07 (d, *J* = 8.1 Hz, 1H, 4H-carbazole), 10.15 (bs, 1H, 9H-carbazole); HRMS calcd for C₂₅H₂₅NO₃ [M + H]⁺ 388.1913, found 388.1912.

Ethyl (E)-3-[8-(1-Adamantyl)-7-hydroxy-9H-carbazol-2-yl]propenoate (68) (method D). Ester **67** (100 mg, 0.20 mmol) after reaction for 2 h, workup, and chromatography (16 to 28% EtOAc/hexane) gave 32 mg (39%) of **68** as a yellow solid: mp 163–166 °C; IR 3392, 2920, 1680, 1242 cm⁻¹; ¹H NMR (acetone-*d*₆) δ 1.39 (t, *J* = 7.2 Hz, 3H, OCH₂CH₃), 1.80–2.00 (m, 6H, AdCH₂), 2.13 (bs, 3H, AdCH), 2.68 (bs, 6H, AdCH₂), 4.25 (q, *J* = 7.2 Hz, 2H, OCH₂CH₃), 5.17 (bs, 1H, OH), 6.51 (d, *J* = 15.9 Hz, 1H, CH=CHCO), 6.86 (d, *J* = 8.4 Hz, 1H, 6H-carbazole), 7.47 (dd, *J* = 8.1, 1.2 Hz, 1H, 3H-carbazole), 7.55 (d, *J* = 1.2 Hz, 1H, 1H-carbazole), 7.77 (d, *J* = 8.4 Hz, 1H, 5H-carbazole), 7.86 (d, *J* = 15.9 Hz, 1H, CH=CHCO), 7.92 (d, *J* = 8.1 Hz, 1H, 4H-carbazole), 8.86 (bs, 1H, 9H-carbazole); HRMS calcd for C₂₇H₂₉NO₃ [M + H]⁺ 416.2220, found 416.2220.

(E)-3-[6-(1-Adamantyl)-7-hydroxy-9H-carbazol-2-yl]propenoic Acid (69). To a suspension of **68** (30 mg, 0.07 mmol) in EtOH (0.2 mL) and THF (0.1 mL) was added 25% aqueous NaOH (50 μL, 0.42 mmol). This mixture was stirred for 24 h, acidified to pH 1 with 1 N HCl (10 mL), and extracted with EtOAc (40 mL, 20 mL). The extract was washed (brine), dried, and concentrated at reduced pressure. The residue was chromatographed (0:50:50 to 9:91:0 MeOH/EtOAc/hexane and then 9:91 to 17:83 MeOH/CH₂Cl₂). The product was washed (pentane) to give 20 mg (74%) of **69** as a yellow solid: mp 184–187 °C; IR 3342, 2907, 1679, 1270 cm⁻¹; ¹H NMR (CD₃OD) δ 1.82–2.02 (m, 6H, AdCH₂), 2.15 (bs, 3H, AdCH), 2.65 (bs, 6H, AdCH₂), 6.56 (d, *J* = 16.2 Hz, 1H, CH=CHCO), 6.72 (d, *J* = 8.1 Hz, 1H, 6H-carbazole), 7.31 (d, *J* = 8.1 Hz, 1H, 3H-carbazole), 7.65 (d, *J* = 16.2 Hz, 1H, CH=CHCO), 7.70 (s, 1H, 1H-carbazole), 7.71 (d, *J* = 8.1 Hz, 1H, 5H-carbazole), 7.85 (d, *J* = 8.1 Hz, 1H, 4H-carbazole); HRMS calcd for C₂₅H₂₅NO₃ [M + H]⁺ 388.1907, found 388.1908.

Computational Studies. Docking Experiments. Docking of analogues to the SHP homology model⁶ derived from the USP LBD–phospholipid complex structure (PDB entry 1G2N) using BioMed Cache version 6.2 (Fujitsu Ltd., Beaverton, OR) was assessed as we previously described.¹⁵ The binding pocket site was derived by selecting all neighboring residues within 4 Å (radius) of the USP ligand 1-stearoyl-2-palmitoylglycerol-3-phosphoethanolamine, which had been docked to the SHP model.⁶ Both the ligand and side chains of pocket residues were allowed to be flexible during the docking process. Final docking poses in Figure 5 were analyzed by measuring interatom distances after overlaying the docked structures by superposing the backbone of the SHP model structure.

CoMFA Experiments. Comparative molecular field analysis (CoMFA) of analogues of 8 substituted at position 3 was performed using SYBYL version 8.0 (Tripos Inc., St. Louis, MO). Three partial CoMFA models were derived from 11 analogues and their IC₅₀ values for inhibiting the viability of three leukemia cell lines (K562, OCI-AML2, and MOLT4). Each initial structure was minimized by the conjugate gradient method and convergence criterion of 0.005 kcal/mol using the Tripos force field with Gasteiger–Huckel charges added. The asterisk-labeled atoms of analogue 47, which had the lowest IC₅₀ values for inhibiting OCI-AML2 and MOLT4 cell viability, comprised the common substructure (Figure S3A of the Supporting Information) used for the alignment. The other 10 analogues were aligned to this template using the database alignment method in SYBYL version 8.0 as shown in Figure S3B of the Supporting Information and placed in a three-dimensional lattice. The steric and electrostatic CoMFA fields were calculated at each lattice intersection of a 2.0 Å spaced grid. An sp³ carbon atom with a formal charge of +1 and a van der Waals radius of 1.52 Å was used as a probe atom to generate Lennard-Jones (steric energies) and Coulombic (electrostatic energies) potential. The van der Waals and Coulombic potentials representing the steric and electrostatic fields, respectively, were calculated using standard Tripos force fields with a distance-dependent dielectric constant of 1.00. Cutoff default values of 30.0 kcal/mol for both steric and electrostatic fields were used.

Biologic Studies. NMR Protein Binding Studies. GST-bound SHP was expressed and purified as described previously.¹⁵ One-dimensional ¹H NMR spectra were recorded with 128 transients and a sweep width of 12376 Hz using a Bruker Avance 600 MHz NMR spectrometer equipped with a TCI cryoprobe so that the sample temperature was maintained at 11 °C. The repetition time was 3 s. Spectra were recorded for solutions of each compound (100 μM 8 and 47 and 200 μM 46) in the bead elution buffer [50 mM Tris (pH 7.2) containing 20 mM reduced glutathione] prepared using 92.5% D₂O and 2% DMSO-*d*₆ alone or with GST-bound SHP (0.5 μM for 8 and 47 and 1.0 μM for 46).

Cell Culture. KG-1 AML cells from H. P. Koeffler (UCLA, Cedars-Sinai Medical Center, Los Angeles, CA) were grown in RPMI 1640 medium supplemented with 5% heat-inactivated fetal bovine serum (FBS) and gentamycin (100 μg/mL). ATRA-resistant HL-60R myeloid leukemia cells from S. Collins (University of Washington, Seattle, WA) were grown under the same conditions. MDA-MB-231 breast cancer cells (ATCC, Manassas, VA) were seeded in DMEM/F-12 medium supplemented with 10% FBS and gentamycin (25 μg/mL). Cells were incubated for 24 h before being treated with compound (final Me₂SO concentration of 0.1%) for 48 or 72 h. K562 AML (ATCC), MOLT4 T-ALL (ATCC), and OCI-AML2 (from S. Kitada, Sanford-Burnham Medical Research Institute) leukemia cell lines were cultured in RPMI 1640 medium (CellGro, Mediatech, Manassas, VA) supplemented with 10% heat-inactivated FBS and a 1% penicillin/streptomycin solution (Omega Scientific, Tarzana, CA) at 37 °C in a 5% CO₂ atmosphere.

Inhibition of Proliferation. KG-1 leukemia cells were seeded in six-well plates containing 3 mL of medium and 5% FBS per well and incubated overnight. After compounds dissolved in Me₂SO were added to provide the designated concentrations, cells were incubated for 48 h and harvested. Cell numbers were determined by counting using a hemocytometer as described previously.¹¹ Results shown are averages of triplicate determinations ± standard deviations (SDs), which were <10%.

Cell Apoptosis. KG-1 leukemia cells were seeded and incubated for 48 h as described for the cell growth inhibition experiments. Apoptotic cells were identified using acridine orange staining for DNA fragmentation as described previously.¹¹ Results shown are the averages of triplicate determinations ± SDs, which were <10%.

Cancer Stem Cell Assay. The effects of compounds on proliferation of MMTV-Wnt1 murine mammary cancer stem cells derived from mammospheres were determined as previously described.¹⁵ Briefly, dissociated cells were plated in MSC medium without serum into gelatin-coated 384-well plates, incubated for 24 h, and then treated with the indicated concentrations of compound in vehicle (final Me₂SO concentration of 0.1%) or vehicle (Me₂SO) alone for 72 h. Cells were fixed and stained with DAPI. Cell numbers were determined by analyzing nine images acquired by the IC100 automatic focusing imaging system and Cyteseer (Vala Sciences, San Diego, CA). Results are expressed as means ± SD from triplicate determinations.

Cell Viability Assay. This assay was conducted as previously reported with several modifications.¹⁵ Briefly, K562, MOLT4, and OCI-AML2 leukemia cell suspensions in medium containing 10% fetal bovine serum (FBS) (1800 cells in 50 μL of medium/well) were added to 384-well white-bottomed Greiner plates and incubated with compounds at the specified concentrations. Compounds were dissolved in Me₂SO (maximal final concentration of 0.1%, which had no effect on cell growth) and then diluted into medium containing 10% FBS. After 72 h at 37 °C, plates were cooled to room temperature for 15 min before luciferase assays were conducted to determine ATP levels using CellTiter Glo Luminescent Cell Viability Reagent (20 μL/well; Promega, Madison, WI) and light emission was measured after 10 min according to the manufacturer's instructions. Experiments were performed in quadruplicate (mean ± SD). Cell viability was calculated on the basis of maximal luminescence intensity observed for each cell line in the presence of the Me₂SO vehicle alone (100% value). Assay results are displayed graphically in Figure S1 of the Supporting Information.

Statistical Analysis. For the data obtained at analogue concentrations of 1.0 and 5.0 μM compared to those of the nontreated control groups, which are given in Tables 1 and 2, the statistical significance between treated and nontreated control groups (*n* = 3 each) was determined by the two-sample *t* test with a degree of freedom (*k*) of 4 on the mean ± standard deviation (SD) data. IC₅₀ values for effects of analogues on the K562, OCI-AML2, and MOLT4 leukemia cell lines were determined from dose–response curves of the means of quadruplicate determinations ± SD, which are shown in Figure S1 of the Supporting Information. The means of the IC₅₀ values ± SD of the effects of compounds on the mammary stem cells that are listed in Table 2 were determined by a one-tailed *t* test on the IC₅₀ values determined from dose–response curves in triplicate experiments. Statistical comparisons between the IC₅₀ value of 8 and those of five other analogues were made using the two-sample *t* test with a degree of freedom (*k*) of 4 on the means ± standard deviation (SD) of their IC₅₀ values. The dose–response curves shown in Figure 3 represent the means of triplicate determinations ± SDs of the effects of analogues on these stem cells.

■ ASSOCIATED CONTENT

Supporting Information

Dose–response curves showing effects of the analogues on ATP levels in K562 AML, OCI-AML2 AML, and MOLT4 T-ALL leukemia cell lines (Figure S1), relationships between logarithms of analogue 3-substituent volumes and logarithms of analogue concentrations that inhibited leukemia cell viability by 50% (Figure S2), physical properties of these substituents at position 3 used for the relationship studies in Figure S2 (Table S1), common substructure used to generate the CoMFA model and the compound alignment (Figure S3), CoMFA model statistics and data used to generate Figure 4 (Tables S2 and S3), HPLC analytical data on target compound purity (Table S4), and the 600 MHz ¹H NMR spectrum of the D₂O used for the binding studies shown in Figure 4A,B (Figure S4). This

material is available free of charge via the Internet at <http://pubs.acs.org>.

AUTHOR INFORMATION

Corresponding Author

*Sanford-Burnham Medical Research Institute, 10901 N. Torrey Pines Rd., La Jolla, CA 92037. Phone: (858) 646-3165. Fax: (858) 646-3197. E-mail: mdawson@sanfordburnham.org.

ACKNOWLEDGMENTS

We are grateful for support of this research by U.S. Public Health Service Grants R01 CA109370 (J.A.F. and M.I.D.) and CA55164 (J.C.R.) and a VA Merit Award (J.A.F.) and to Dr. Roberto Pellicciari (University of Perugia, Perugia, Italy) for use of the USP LBD-derived homology model of SHP.

ABBREVIATIONS

1-Ad, 1-adamantyl; 3-Cl-AHPC, (*E*)-4-[3'-(1-adamantyl)-4'-hydroxyphenyl]-3-chlorocinnamic acid; AHPN, 6-[3'-(1-adamantyl)-4'-hydroxyphenyl]-2-naphthalenecarboxylic acid; AML, acute myelocytic leukemia; ATRA, all-*trans*-retinoic acid; CML, chronic myeloid leukemia; CoMFA, comparative molecular field analysis; DAPI, 4',6-diamidino-2-phenylindole dihydrochloride; RAR, retinoic acid receptor; RXR, retinoid X receptor; SHP, small heterodimer partner; T-ALL, T-cell acute lymphoblastic leukemia

REFERENCES

- (1) Farhana, L.; Dawson, M. I.; Leid, M.; Wang, L.; Moore, D. D.; Liu, G.; Xia, Z.; Fontana, J. A. Adamantyl-substituted retinoid-related molecules bind small heterodimer partner and modulate the Sin3A repressor. *Cancer Res.* **2007**, *67*, 318–325.
- (2) Zhang, Y.; Soto, J.; Park, K.; Viswanath, G.; Kuwada, S.; Abel, E. D.; Wang, L. Nuclear receptor SHP, a death receptor that targets mitochondria, induces apoptosis and inhibits tumor growth. *Mol. Cell. Biol.* **2010**, *30*, 1341–1356.
- (3) Zhang, Y.; Wang, L. Nuclear receptor SHP inhibition of Dnmt1 expression via ERR γ . *FEBS Lett.* **2011**, *585*, 1269–1275.
- (4) Kim, M.-K.; Chanda, D.; Lee, I.-K.; Choi, H.-S.; Park, K.-G. Targeting orphan nuclear receptor SHP in the treatment of metabolic diseases. *Expert Opin. Ther. Targets* **2010**, *14*, 453–466.
- (5) Billas, I. M.; Moulinier, L.; Rochel, N.; Moras, D. Crystal structure of the ligand-binding domain of the ultraspiracle protein USP, the ortholog of retinoid X receptors in insects. *J. Biol. Chem.* **2001**, *276*, 7465–7474.
- (6) Macchiariulo, A.; Rizzo, G.; Costantino, G.; Fiorucci, S.; Pellicciari, R. Unveiling hidden features of orphan nuclear receptors: The case of the small heterodimer partner (SHP). *J. Mol. Graphics Modell.* **2006**, *24*, 362–372.
- (7) Cellanetti, M.; Gunda, V.; Wang, L.; Macchiariulo, A.; Pellicciari, R. Insights into the binding mode and mechanism of action of some atypical retinoids as ligands of the small heterodimer partner (SHP). *J. Comput.-Aided Mol. Des.* **2010**, *24*, 943–956.
- (8) Farhana, L.; Dawson, M. I.; Dannenberg, J.-H.; Xu, L.; Fontana, J. A. SHP and Sin3A expression are essential for adamantyl-substituted retinoid-related molecule-mediated nuclear factor- κ B activation, c-Fos/c-Jun expression, and cellular apoptosis. *Mol. Cancer Ther.* **2009**, *8*, 1625–1635.
- (9) Farhana, L.; Dawson, M. I.; Xia, Z.; Aboukameel, A.; Xu, L.; Liu, G.; Das, J. K.; Hatfield, J.; Levi, E.; Mohammad, R.; Fontana, J. A. Adamantyl-substituted retinoid-related molecules induce apoptosis in human acute myelogenous leukemia cells. *Mol. Cancer Ther.* **2010**, *9*, 2903–2913.
- (10) Farhana, L.; Dawson, M. I.; Murshed, F.; Fontana, J. A. Maximal adamantyl-substituted retinoid-related molecule-induced apoptosis

requires NF- κ B noncanonical and canonical pathway activation. *Cell Death Differ.* **2011**, *18*, 164–173.

(11) Dawson, M. I.; Harris, D. L.; Liu, G.; Hobbs, P. D.; Lange, C. W.; Jong, L.; Bruey-Sedano, N.; James, S. Y.; Zhang, X.-K.; Peterson, V. J.; Leid, M.; Farhana, L.; Rishi, A. K.; Fontana, J. A. Antagonist analogue of 6-[3'-(1-adamantyl)-4'-hydroxyphenyl]-2-naphthalenecarboxylic acid (AHPN) family of apoptosis inducers that effectively blocks AHPN-induced apoptosis but not cell-cycle arrest. *J. Med. Chem.* **2004**, *47*, 3518–3536.

(12) Klaholz, B. P.; Renaud, J.-P.; Mitschler, A.; Zusi, C.; Chambon, P.; Gronemeyer, H.; Moras, D. Conformational adaptation of agonists to the human nuclear receptor RAR γ . *Nat. Struct. Biol.* **1998**, *5*, 199–202.

(13) Dawson, M. I.; Xia, Z.; Jiang, T.; Ye, M.; Fontana, J. A.; Farhana, L.; Patel, B.; Xue, L. P.; Bhuiyan, M.; Pellicciari, R.; Macchiariulo, A.; Nuti, R.; Zhang, X.-K.; Han, Y.-H.; Tautz, L.; Hobbs, P. D.; Jong, L.; Waleh, N.; Chao, W.-R.; Feng, G.-S.; Pang, Y.; Su, Y. Adamantyl-substituted retinoid-derived molecules that interact with the orphan nuclear receptor small heterodimer partner: Effects of replacing the 1-adamantyl or hydroxyl group on inhibition of cancer cell growth, induction of cancer cell apoptosis, and inhibition of SRC homology 2 domain-containing protein tyrosine phosphatase-2 activity. *J. Med. Chem.* **2008**, *51*, 5650–5662.

(14) Heck, R. F.; Nolley, J. P. Jr. Palladium-catalyzed vinylic hydrogen substitution reactions with aryl, benzyl, and styryl halides. *J. Org. Chem.* **1972**, *37*, 2320–2322.

(15) Xia, Z.; Farhana, L.; Correa, R. G.; Das, J. K.; Castro, D. J.; Yu, J.; Oshima, R. G.; Reed, J. C.; Fontana, J. A.; Dawson, M. I. Heteroatom-substituted analogues of orphan nuclear receptor small heterodimer partner ligand and apoptosis inducer (*E*)-4-[3-(1-adamantyl)-4-hydroxyphenyl]-3-chlorocinnamic acid. *J. Med. Chem.* **2011**, *54*, 3793–3816.

(16) Wittig, G.; Schöllkopf, U. Über Triphenyl-phosphin-methylene als olefinbildende Reagenzien. *Chem. Ber.* **1954**, *87*, 1318.

(17) Miyaura, N.; Suzuki, A. Palladium-catalyzed cross-coupling reactions of organoboron compounds. *Chem. Rev.* **1995**, *95*, 2457–2483.

(18) Freeman, A. W.; Urvoy, M.; Criswell, M. E. Triphenylphosphine-mediated reductive cyclization of 2-nitrophenyls: A practical and convenient synthesis of carbazoles. *J. Org. Chem.* **2005**, *70*, 5014–5019.

(19) Naffziger, M. R.; Ashburn, B. O.; Perkins, J. R.; Carter, R. G. Diels-Alder approach for the construction of halogenated, o-nitro biaryl templates and application to the total synthesis of the anti-HIV agent siamenol. *J. Org. Chem.* **2007**, *72*, 9857–9865.

(20) Shao, Z. M.; Dawson, M. I.; Li, X. S.; Rishi, A. K.; Sheikh, M. S.; Han, Q. X.; Ordonez, J. V.; Shroot, B.; Fontana, J. A. p53 independent G₀/G₁ arrest and apoptosis induced by a novel retinoid in human breast cancer cells. *Oncogene* **1995**, *11*, 493–504.

(21) Tang, X. H.; Gudas, L. J. Retinoids, retinoic acid receptors, and cancer. *Annu. Rev. Pathol.* **2011**, *6*, 345–364.

(22) Gieseler, F.; Bauer, E.; Nuessler, V.; Clark, M.; Valsamas, S. Molecular effects of topoisomerase II inhibitors in AML cell lines: Correlation of apoptosis with topoisomerase II activity but not with DNA damage. *Leukemia* **1999**, *13*, 1859–1863.

(23) Qi, H.; Ratnam, M. Synergistic induction of folate receptor β by all-*trans* retinoic acid and histone deacetylase inhibitors in acute myelogenous leukemia cells: Mechanism and utility in enhancing selective growth inhibition by antifolates. *Cancer Res.* **2006**, *66*, 5875–5882.

(24) Drach, J.; Lopez-Berestein, G.; McQueen, T.; Andreeff, M.; Mehta, K. Induction of differentiation in myeloid leukemia cell lines and acute promyelocytic leukemia cells by liposomal all-*trans*-retinoic acid. *Cancer Res.* **1993**, *53*, 2100–2104.

(25) Zhang, Y.; Dawson, M. I.; Ning, Y.; Polin, L.; Parchment, R. E.; Corbett, T.; Mohamed, A. N.; Feng, K.-C.; Farhana, L.; Rishi, A. K.; Hogge, D.; Leid, M.; Peterson, V. J.; Zhang, X.-K.; Mohammad, R.; Lu, J.-S.; Willman, C.; VanBuren, E.; Biggar, S.; Edelman, M.; Eilender, D.; Fontana, J. A. Induction of apoptosis in retinoid-refractory acute myelogenous leukemia by a novel AHPN analog. *Blood* **2003**, *102*, 3743–3752.

- (26) Schmelz, K.; Sattler, N.; Wagner, M.; Lubbert, M.; Dorken, B.; Tamm, I. Induction of gene expression by 5-aza-2'-deoxycytidine in acute myeloid leukemia (AML) and myelodysplastic syndrome (MDS) but not epithelial cells by DNA-methylation-dependent and -independent mechanisms. *Leukemia* **2005**, *19*, 103–111.
- (27) Zhou, H. R.; Shen, J. Z.; Fu, H. Y.; Ye, B. G.; Fan, L. P.; Lin, F. A. Detection of promoter methylation of p16 gene in hematological malignant cell lines by nested methylation specific polymerase chain reaction. *Zhongguo Shi Yan Xue Ye Xue Za Zhi* **2006**, *14*, 375–378.
- (28) Koeffler, H. P.; Golde, D. W. Human myeloid leukemia cell lines: A review. *Blood* **1980**, *56*, 344–350.
- (29) Ekiz, H. A.; Can, G.; Gunduz, U.; Baran, Y. Nilotinib significantly induces apoptosis in imatinib-resistant K562 cells with wild-type BCR-ABL, as effectively as in parental sensitive counterparts. *Hematology* **2010**, *15*, 33–38.
- (30) Tang, X. Y.; Wang, C. H.; Xiao, G. F. The effect of ATRA-induced leukemic cell differentiation on Brd7 gene expression in leukemia cell lines. *Zhongguo Shi Yan Xue Ye Xue Za Zhi* **2010**, *18*, 593–596.
- (31) Jimi, S.; Mashima, K.; Matsumoto, T.; Hara, S.; Suzumiya, J.; Tamura, K. RAR α is a regulatory factor for Am-80-induced cell growth inhibition of hematologic malignant cells. *Int. J. Oncol.* **2007**, *31*, 397–404.
- (32) Lee, H. J.; Thompson, J. E.; Wang, E. S.; Wetzler, M. Philadelphia chromosome-positive acute lymphoblastic leukemia: Current treatment and future perspectives. *Cancer* **2011**, *117*, 1583–1594.
- (33) Ru, H. Y.; Chen, R. L.; Lu, W. C.; Chen, J. H. hBUB1 defects in leukemia and lymphoma cells. *Oncogene* **2002**, *21*, 4673–4679.
- (34) Rodrigues, N. R.; Rowan, A.; Smith, M. E.; Kerr, I. B.; Bodmer, W. F.; Gannon, J. V.; Lane, D. P. p53 mutations in colorectal cancer. *Proc. Natl. Acad. Sci. U.S.A.* **1990**, *87*, 7555–7559.
- (35) Yamaguchi, T.; Katoh, I.; Kurata, S. Azidothymidine causes functional and structural destruction of mitochondria, glutathione deficiency and HIV-1 promoter sensitization. *Eur. J. Biochem.* **2002**, *269*, 2782–2788.
- (36) Hakimelahi, G. H.; Ly, T. W.; Yu, S.-F.; Zakerinia, M.; Khalafi-Nezhad, A.; Soltani, M. N.; Gorgani, M. N.; Chadegani, A. R.; Moosavi-Movahedi, A. A. Design and synthesis of a cephalosporin-retinoic acid prodrug activated by a monoclonal antibody- β -lactamase conjugate. *Bioorg. Med. Chem.* **2001**, *9*, 2139–2147.
- (37) Anuchapreeda, S.; Tima, S.; Duangrat, C.; Limtrakul, P. Effect of pure curcumin, demethoxycurcumin, and bisdemethoxycurcumin on WT1 gene expression in leukemic cell lines. *Cancer Chemother. Pharmacol.* **2008**, *62*, 585–594.
- (38) Sugiyama, H. Cancer immunotherapy targeting Wilms' tumor gene WT1 product. *Expert Rev. Vaccines* **2005**, *4*, 503–512.
- (39) Ochsenreither, S.; Fusi, A.; Busse, A.; Bauer, S.; Scheibenbogen, C.; Stather, D.; Thiel, E.; Keilholz, U.; Letsch, A. "Wilms Tumor Protein 1" (WT1) peptide vaccination-induced complete remission in a patient with acute myeloid leukemia is accompanied by the emergence of a predominant T-cell clone both in blood and bone marrow. *J. Immunother.* **2010**, *34*, 85–91.
- (40) Lu, Y.; Shi, T.; Wang, Y.; Yang, H.; Yan, X.; Luo, X.; Jiang, H.; Zhu, W. Halogen bonding: A novel interaction for rational drug design? *J. Med. Chem.* **2009**, *52*, 2854–2862.
- (41) Bissantz, C.; Kuhn, B.; Stahl, M. A medicinal chemist's guide to molecular interactions. *J. Med. Chem.* **2010**, *53*, 5061–5084.
- (42) Scheiner, S.; Kar, T.; Pattanayak, J. Comparison of various types of hydrogen bonds involving aromatic amino acids. *J. Am. Chem. Soc.* **2002**, *124*, 13257–13264.
- (43) Kovacs, A.; Varga, Z. Halogen acceptors in hydrogen bonding. *Coord. Chem. Rev.* **2006**, *250*, 710–727.
- (44) Dawson, M. L.; Xia, Z.; Liu, G.; Ye, M.; Fontana, J. A.; Farhana, L.; Patel, B. B.; Arumugarajah, S.; Bhuiyan, M.; Zhang, X.-K.; Han, Y.-H.; Stallcup, W. B.; Fukushi, J.; Mustelin, T.; Tautz, L.; Su, Y.; Harris, D. L.; Waleh, N.; Hobbs, P. D.; Jong, L.; Chao, W. R.; Schiff, L. J.; Sani, B. P. An adamantyl-substituted retinoid-derived molecule that inhibits cancer cell growth and angiogenesis by inducing apoptosis and binds to small heterodimer partner nuclear receptor: Effects of modifying its carboxylate group on apoptosis, proliferation, and protein-tyrosine phosphatase activity. *J. Med. Chem.* **2007**, *50*, 2622–2639.
- (45) Mcbee, E. T.; Pierce, O. R.; Lowery, R. D.; Rapkin, E. Some dihalo-(trifluoromethyl)benzenes. *J. Am. Chem. Soc.* **1951**, *73*, 3932–3934.
- (46) Dabrowski, M.; Kubicka, J.; Lulinski, S.; Serwatowski, J. Halogen-lithium exchange between substituted dihalobenzenes and butyllithium: Application to the regioselective synthesis of functionalized bromobenzaldehydes. *Tetrahedron* **2005**, *61*, 6590–6595.
- (47) Molinspiration Chemoinformatics, Slovensky Grob, Slovak Republic. <http://www.molinspiration.com/cgi-bin/properties> (accessed February 8, 2011).